Commission of the European Community

JOINT
RESEARCH
CENTRE

NEANDC (E) 282 "U" Vol. III Euratom
INDC (EUR) 021/G

ANNUAL PROGRESS REPORT ON NUCLEAR DATA
1986

CENTRAL BUREAU FOR NUCLEAR MEASUREMENTS

GEEL (BELGIUM)

June 1987

Commission of the European Community

JOINT
RESEARCH
CENTRE

NEANDC (E) 282 "U" Vol. III Euratom
INDC (EUR) 021/G

ANNUAL PROGRESS REPORT ON NUCLEAR DATA
1986

CENTRAL BUREAU FOR NUCLEAR MEASUREMENTS

GEEL (BELGIUM)

June 1987

TABLE OF CONTENTS

Editing: H.H. Hansen

Note: For further information concerning the Project Nuclear Measurements (Nuclear Data, Nuclear Metrology), please contact A.J. Deruytter, Project Manager.

EXECUTIVE SUMMARY

A.J. Deruytter

In the 1984-1987 multiannual research programme of CBNM, JRC-Geel, the project Nuclear Measurements is concerned with Nuclear Data and Nuclear Metrology.

In the reporting period 1986 efforts for the improvement of the set of standard neutron cross-sections and other quantities selected within the INDC/NEANDC Standards File have continued. The effort went mainly to neutron data and in particular to the ^{235}U fission cross-section standard and the standard fission neutron spectrum of ^{252}Cf. Also the evaluation of the thermal constants of the common fissile nuclides and the fission neutron yield of ^{252}Cf was finalized.

In the field of nuclear data for fission technology work was concentrated on European Requests in the NEA High Priority Request List. Attention went to measurements of actinide data in the subthermal neutron energy range, a measurement of the fission cross-section of ^{243}Am and measurements in connection with the NEANDC task force on the 1.15 keV resonance in ^{56}Fe.

The measurements for fusion technology aimed at the improvement of relevant and important neutron data in particular for neutron transport calculations in the blanket which contains lithium as a titrium breeder material and for prediction of gas production. Measurements on the resonance structure in the ^{28}Si + n and ^{207}Pb + n systems have also yielded important physical information.

The radionuclide task followed three lines: determination of decay-scheme data, preparation of special standards and the improvement of measurement techniques including international comparisons. A measurement of the alpha-particle emission probabilities in the ^{237}Np decay was performed and CBNM participated in an international comparison of activity-concentration measurements of a ^{109}Cd solution, organized by BIPM, Paris.

In the field of metrology of neutron flux and dose CBNM participated in international comparisons of neutron fluence rates (1) at 565 keV, organized by NPL, Teddington and (2) at several energies via fission fragment counting with ionization chambers, organized by AERE, Harwell. The characteristic parameters of the CBNM graphite calorimeter were determined experimentally and the tissue-equivalent plastic (TEP) calorimeter was put into operation.

1 NUCLEAR DATA

1.1 NUCLEAR DATA FOR STANDARDS

Nuclear data for standards comprise mainly neutron data and in particular the ^{235}U fission cross-section standard and the standard fission spectrum of ^{252}Cf, of which the results are described in some detail below. The evaluation of radionuclide decay data, in particular X- and γ-ray detector calibration data, in the framework of an IAEA coordinated research programme was started. It concerns the evaluation of the γ-ray emission probabilities of ^{228}Th, ^{239}Np, ^{241}Am and ^{243}Am. Also the evaluation of X-ray emission probabilities, and in collaboration with LMRI, that of the internal conversion data of 33 radionuclides are in progress.

1.1.1 Neutron Data for Standards

$^{235}U(n,f)$ Fragment Mass, Angle, and Kinetic Energy Distributions for Thermal $\leq E_n < 0.5$ MeV

F.-J. Hambsch*, H.-H. Knitter, C. Budtz-Jørgensen, R. Vogt, H. Bax
(WRENDA request N° 781192R)

Fission properties like fragment mass- and kinetic-energy distributions of thermal and high energy (> 0.5 MeV) neutron induced fission of ^{235}U are rather well known[1,2]. For the understanding of the fission process in the low and medium neutron-energy range (eV to ~ 0.5 MeV) the changes of these properties with the excitation energy of the compound nucleus ^{236}U and with the resonance spin ($J = 3^-, 4^-$ for s-wave neutrons), are of interest. No systematic measurement has been done in this energy region in the past. Therefore the fragment mass, kinetic-energy and angular distributions of $^{235}U(n,f)$ were measured at the Geel electron linear accelerator (GELINA), as function of incident neutron energy from thermal to 0.5 MeV. The experiment was set up at about 9 m from the GELINA target. The experimental and electronic arrangements were already shown in the previous progress report[3]. As fission-fragment detector, a Frisch gridded

---

* EC Fellow

(1) W.Lang, H.G. Clerc, H. Wohlfarth, H. Schrader and K.H. Schmidt, Nucl. Phys. A345 (1980) 34

(2) Ch.A.Straede, Ph. D. Thesis, Commission of the European Communities, Central Bureau for Nuclear Measurements, Geel, Belgium, May 1985

(3) NEANDC (E) 272 "U" Vol. III Euratom; INDC (EUR) 020/G (1986), p.6

ionization chamber has been used. A compensation technique has been applied by the use of an unloaded ionization chamber to compensate for the signals induced by the GELINA γ-ray flash, to prevent a disturbance of the measured fission parameters. A $^{235}UF_4$ layer of ~ 47 μg/cm^2 thickness and 7 cm diameter was used. It was on a polyimide backing and covered by ~ 80 μg/cm^2 Au to ensure electrical conductivity.

The neutron energy was determined by a time-of-flight technique using a time coder with 4 ns channel width. The timing signal was obtained from the cathode of the ionization chamber which was operated as a flow chamber with a gas pressure of 10^5 Pa of 90% Ar with 10% CH_4. From the anode signals the energies of the two fragments are obtained, whereas the sum signals of the respective grids and anodes are energy and angle dependent. Both signals together allow the determination of the cosine of the fragment-emission angle with respect to the neutron-beam direction.

Both high (800 Hz) and low (40 Hz) repetition frequencies at GELINA were used and the data acquisition has been finished. The advantage of the low frequency was that the neutron-energy range could be extended to thermal. Approximately $1.3 \cdot 10^7$ fission events for neutron energies between 1 eV and 0.5 MeV were recorded. Measurements with thermal neutrons, produced by thermalization in a paraffin $(CH_2)_n$ block positioned in front of the detector, served as a reference.

Angular Distribution

In Fig. 1 the angular anisotropies W(0°)/W(90°)-1 are shown as a function of neutron energy between 0 and 0.5 MeV in comparison with previous measurements[1,2]. For the first time this neutron-energy range was covered in one experiment. The theoretical calculations, which are presented by the dashed lines in Fig. 1 can reproduce the negative anisotropies under the restrictive assumption that either R-(eigen-value r = + 1) or S-(eigen-value s = + 1) invariance of the fissioning system at the saddle point is fulfilled. S-invariance would be in agreement with a suggestion of Bohr that the nucleus is pear-shaped at the saddle point. Moreover, the experiment reveals that the K-quantum number is very neutron energy dependent in this range.

---

(1) A.R. de L. Musgrove, J.W. Boldeman, J.L. Cook, D.W. Lang, E.K. Rose, R.L. Walsh, J. Caruana and J.N. Mathur, J. Phys. G: Nucl. Phys. 7 (1981) 549.

(2) J.W. Meadows and C. Budtz-Jørgensen, Nuclear Data and Measurement Series, ANL/NDM-64 (1982)

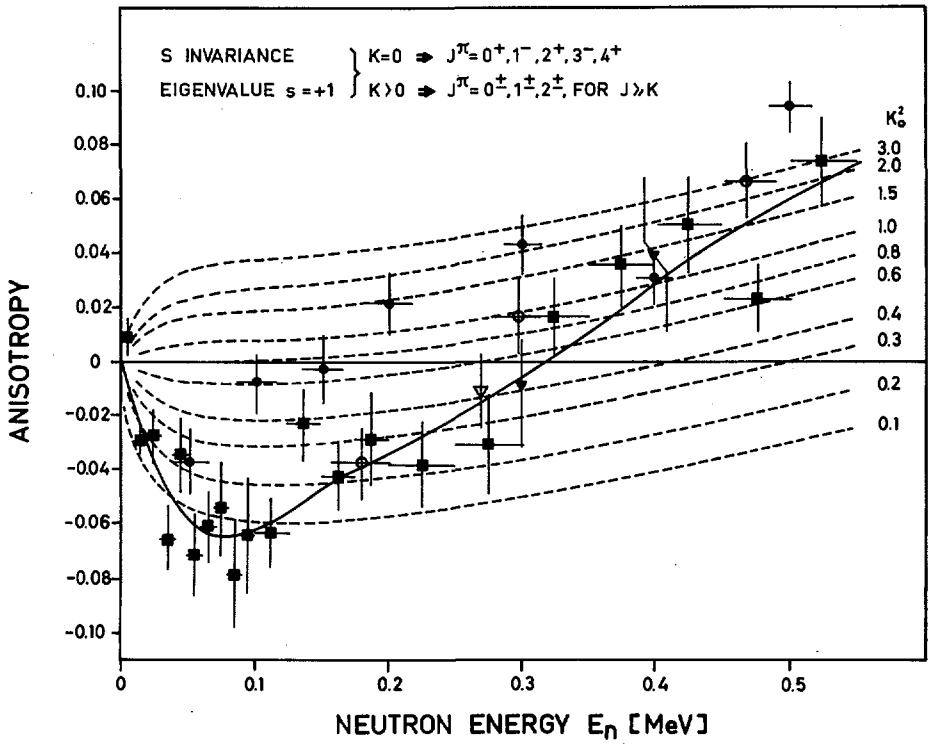

Fig. 1. Fission fragment angular anisotropy for $^{235}U(n,f)$ as function of neutron energy. The full line is an eye-guide through the present experimental points represented by the full square symbols

Total Kinetic Energy as Function of E_n in the Resolved Resonance Region

The "channel theory" of fission from A. Bohr[1] expects differences in the fragment mass- and total kinetic energy distributions depending on the resonance spin (^{235}U : 3^- or 4^-). Experiments performed in the resonance energy region e.g. asymmetric to symmetric mass ratios[2] could not clearly verify the above mentioned assumptions because of lack of spin assignments. In the upper part of Fig. 2 the difference of the average total kinetic energy (TKE) relative to the thermal value is shown as function of the incident neutron energy. In the lower part the relative number of prompt fission neutrons $\bar{\nu}_p$ measured by R.E. Howe et al.[3] are plotted in the same energy intervals. The measured TKE in most cases is higher than that for thermal neutron induced fission and tends to be anticorrelated with $\bar{\nu}_p(E)$ as expected from energy balance considerations. However, although both spin states are involved in the data shown in Fig. 2, no significant spin dependence of the average TKE could be found. The measured mass distributions can be described by a fit of five Gaussian distributions (Fig. 3). The ratio of the weights, W_1/W_2, from the Gaussian

(1) A. Bohr, Proc. First Int. Conf. on the Peaceful Uses of Atomic Energy, P 1911, Vol 2 (1956) 151, United Nations, New York

(2) G. Cowan, B. Bayhurst, R. Prestwood, J. Gilmore and G. Knobeloch, Phys. Rev. C2 (1970) 615

(3) R.E. Howe, T.W. Phillips and C.D. Bowman, Phys. Rev. C13 (1976) 195

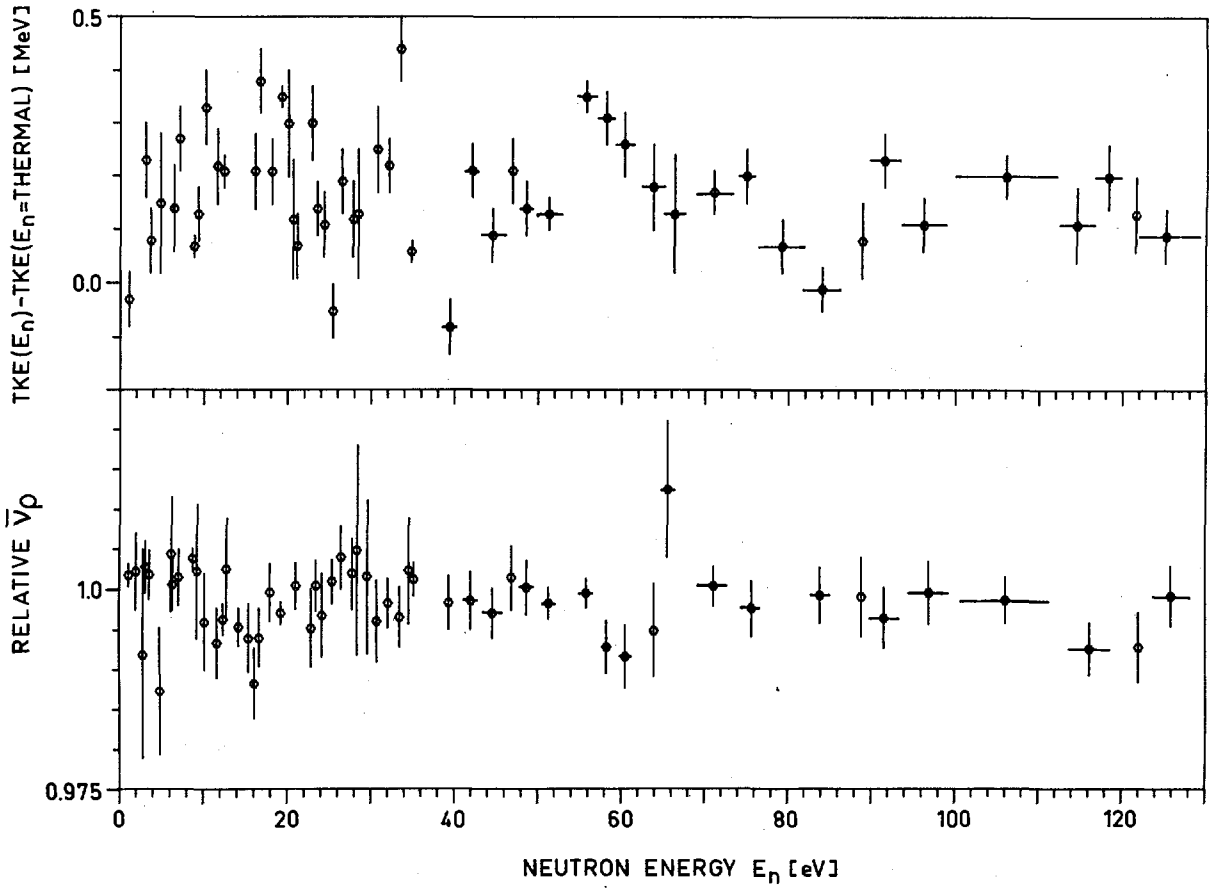

Fig. 2. Upper part: difference of the presently measured average total kinetic energy relative to the thermal value. Lower part: relative number of prompt fission neutrons as function of incident neutron energy from R.E. Howe et al.[1]

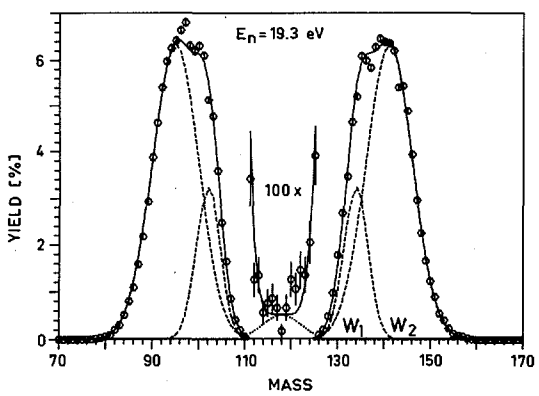

Fig. 3. Experimental fragment mass distributions fitted with 5 Gaussian functions indicated by the dashed lines

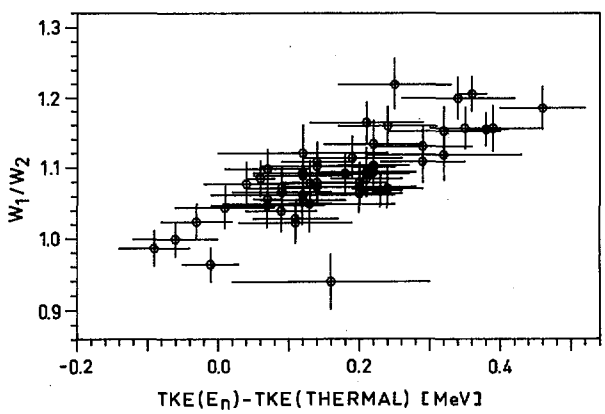

Fig. 4. Measured average TKE compared to relative weights W_1/W_2 of the asymmetric Gaussian distributions in Fig. 3

(1) R.E. Howe, T.W. Phillips and C.D. Bowman, Phys. Rev. C13 (1976) 195

distributions associated with the asymmetric mass peak relative to thermal shows a strong correlation with the measured TKE values (Fig. 4). This can be understood, because the mass distribution relative to thermal shows drastic changes as can be seen for two strong resonances in Fig. 5, where

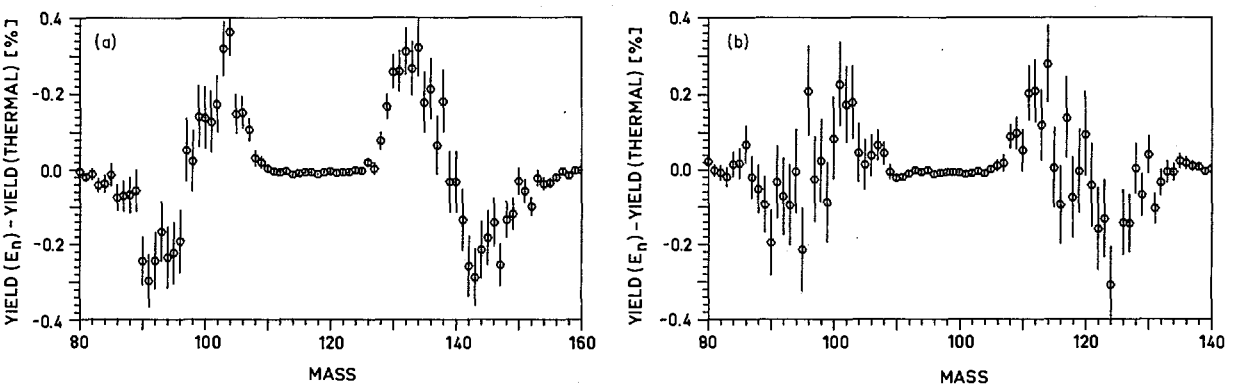

Fig. 5. Changes in the mass distribution relative to thermal (a) 19.3 eV, $J^{\pi} = 4^-$; (b) 12.4 eV, $J^{\pi} = 3^-$

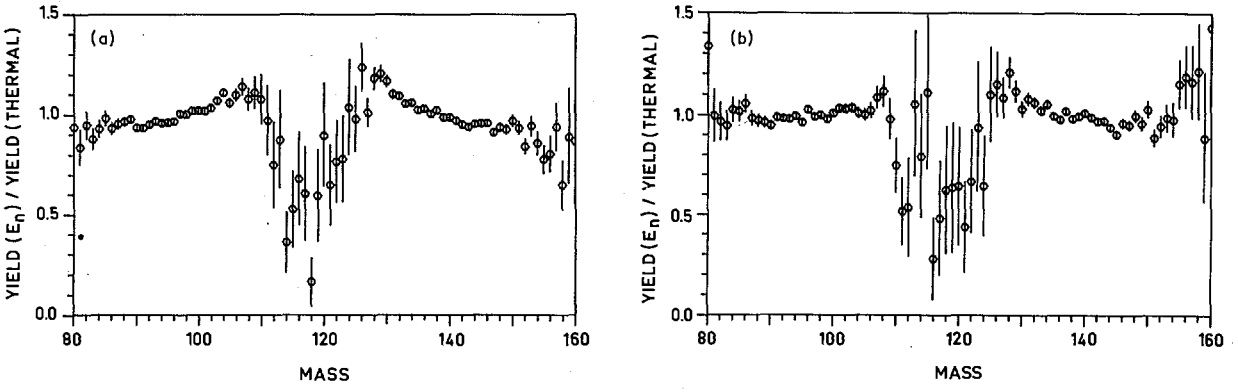

Fig. 6. Changes in the symmetric mass region relative to thermal (a) 19.3 eV, $J^{\pi} = 4^-$; (b) 12.4 eV, $J^{\pi} = 3^-$

the asymmetric mass peaks have been shifted towards more symmetric masses. On the other hand, the symmetric yield for both resonances, even with different spin states, has dropped compared to the thermal yield by nearly a factor of two as seen in Fig. 6. However, also in the ratio of asymmetric to symmetric fission yields no spin dependence could be observed.

The description of the mass distribution by means of three Gaussians is qualitatively in agreement with the fission mode-theory of U. Brosa et al.[1], who can explain the observed asymmetric mass distribution by means of three different paths in the potential energy landscape of ^{235}U.

---

(1) U. Brosa, S. Grossmann and A. Müller, Int. Symp. on Nucl. Physics, Gaussig, GDR, November 1986

Investigation of the Spontaneous Fission of ^{252}Cf

C. Budtz-Jørgensen, H.-H. Knitter
(WRENDA request N°s 792189 R, 821026 R)

The neutron energy spectrum of the spontaneous fission of ^{252}Cf is regarded as a neutron spectrum shape standard. This standard is widely used for neutron detector calibration purposes. It is however not clear with which mathematical parametrization the spectrum can be best described, especially at higher neutron energies. Therefore more detailed experimental effort is needed to obtain a realistic, theory based spectrum-shape description.

A multi-parameter experiment for a detailed study of the prompt fission neutron spectrum was set up. Fission-fragment detection is done using the gridded twin ionization chamber developed at CBNM with which the fission fragment angle, nuclear charge, and the kinetic energy of the two fission fragments are measured in a 2π geometry. The time information of the fission events is obtained from the common cathode giving a time-resolution of better than 0.7 ns. The neutron detector is located on the axis of the ionization chamber, at a distance of 0.52 m from the ^{252}Cf source. Neutron energies are determined using the time-of-flight technique. Both, the pulse height as well as the pulse shape for n/γ discrimination are recorded in order to distinguish between γ-ray and neutron emission in the fission process. For each fission event where a neutron is detected, all parameters are measured simultaneously. They are digitized and stored sequentially on magnetic tape for off-line analysis. The double energy information is used to derive the fission fragment masses. For cold fragmentation a mass resolution of 0.5 u is observed corresponding to a kinetic-energy resolution of less than 0.5 MeV.

The grid signals of the twin ionization chamber are energy, angle, mass and also nuclear charge dependent. The fragment-angle information can be obtained as the cosine of the angle θ between fragment direction and chamber-symmetry axis. The $\cos\theta$ resolution is typically 0.05. A technique using both the anode and the grid signals was developed to extract the information on the nuclear charge number Z of the fission fragment. The charge resolution of the method ($\Delta Z/Z \simeq 1/40$, $Z = 46$) is sufficient for determination of charge distributions in fission. The above experimental set-up thus in principle allows a determination of the ^{252}Cf fission neutron spectrum, $N(E_n;\ A,\ Z,\ \theta)$ versus fragment mass and atomic number and versus the angle between fragment and neutron directions. Some first results are given below.

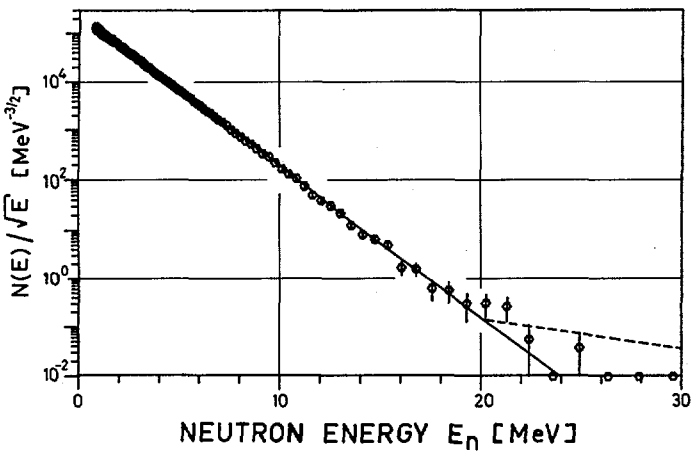

Fig. 7. Fission neutron energy spectrum of ^{252}Cf divided by $\sqrt{E}$ versus the neutron energy E_n

A preliminary evaluation of the mass-integrated prompt fission neutron spectrum of $^{252}Cf(sf)$ has been made. The spontaneous fission process is not only accompanied by neutrons but also by γ rays which might be detected by the neutron detector. Most of the γ-ray emission occurs at the instant of scission and up to a few ns later. In this time interval also the highly energetic neutrons are emitted with a very low intensity. In the present evaluation special attention was given to avoid interference of the γ-rays with the neutrons. The neutron spectrum divided by $\sqrt{E}$ is plotted in Fig. 7 versus the neutron energy. The full line in Fig. 7 represents the result of a least squares fit through the experimental data using a Maxwellian energy distribution. This preliminary neutron-energy spectrum shows no major deviations from the Maxwell distribution in the neutron-energy range from 0.8 MeV to 20 MeV. The deviations from the Maxwell distribution are in general less than 5% in the above-mentioned range. The dashed line corresponds to the experimental spectrum measurements of Märten et al.[1], who found a large excess of neutrons above 20 MeV. The presently evaluated data neither confirm nor contradict the measured excess of neutrons. From the angular distributions averaged over all fragments the intensity ratio N(90°)/N(0°) was evaluated as function of the neutron energy and is plotted in Fig. 8. The present data agree fairly well with early results of Bowman et al.[2] below 4 MeV. However, at higher neutron energies the data are much more anisotropic. The intensity ratios N(90°)/N(0°) are more than one order of magnitude smaller than those of Bowman et al.[2] above 8 MeV. The full line in Fig. 8 represents calculations of the angular anisotropy as function of the

(1) H. Märten, D. Seeliger, and B. Strobinski, Proc. Int. Conf. Nucl. Data for Sci. and Techn., Reidel Publ. Co, NL, (1982), p. 488

(2) H.R. Bowman, S.G. Thompson, J.C.D. Milton and W.J. Swiatecki, Phys. Rev. 126 (1962) 2120

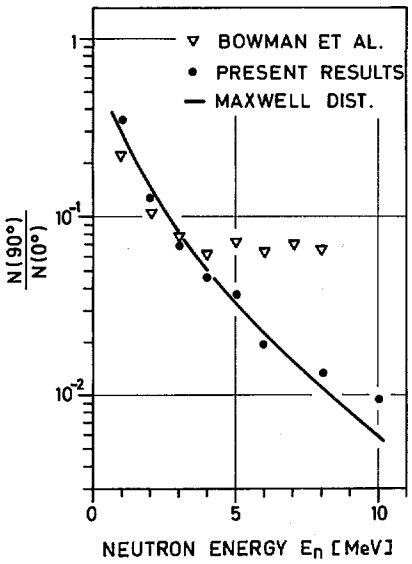

Fig. 8. Neutron intensity ratio N(90°)/N(0°) versus the neutron energy

neutron energy with the assumption that all neutrons are emitted from the fully accelerated fragments. The energy dependence of the present N(90°)/N (0) results agree with the assumption that all neutrons are emitted from the fully accelerated fragments. The existence of a hard (T = 2.0 - 2.5 MeV) scission neutron component which Märten[1] concluded from the Bowman et al.[2] angular distributions must be refuted. A more thorough analysis of the angular distributions is needed in order to decide whether perhaps a soft component of scission neutrons is present.

For the determination of the neutron spectrum as function of the fragment properties a detailed knowledge of the fragment distributions with respect to mass and atomic number as well as to the total kinetic energy, TKE, is needed. Therefore, a measurement of these distributions for ^{252}Cf(sf) was performed with the above mentioned chamber aiming at high accuracy (~ $5 \cdot 10^7$ recorded fission events). New and interesting results were obtained in the region of high TKE where the Q values are nearly exhausted. Fig. 9 shows the present yield/fission for TKE close to the maximum Q-values. The latter quantity is shown as a thick line calculated from the mass tables. In the range A_L = 102-112 and for A_L = 120 the highest measured TKE lie within about 1 MeV of the Q_{max} line. In the range A_L = 102-112 the light and heavy fragments are stabilized by the N ~ 66 and N ~ 86 deformed neutron shells, respectively. The mass split 120/132 is favoured by the double magic $^{132}Sn_{50}$ heavy fragment. The TKE lines show clearly fine structures with a period of ~ 5 u which can be attributed to favoured fragmentation into even charged fragments.

Using the above described method the fragment nuclear charges could be determined for all fission events for which the TKE is larger than the values given by the dash-dotted line in Fig. 9. The lower part of the

(1) H. Märten, Proc. IAEA Consultants' Meeting, Smolenice, INDC(NDS)-146, (1983), p. 195

(2) H.R. Bowman, S.G. Thompson, J.C.D. Milton and W.J. Swiatecki, Phys. Rev. 126 (1962) 2120

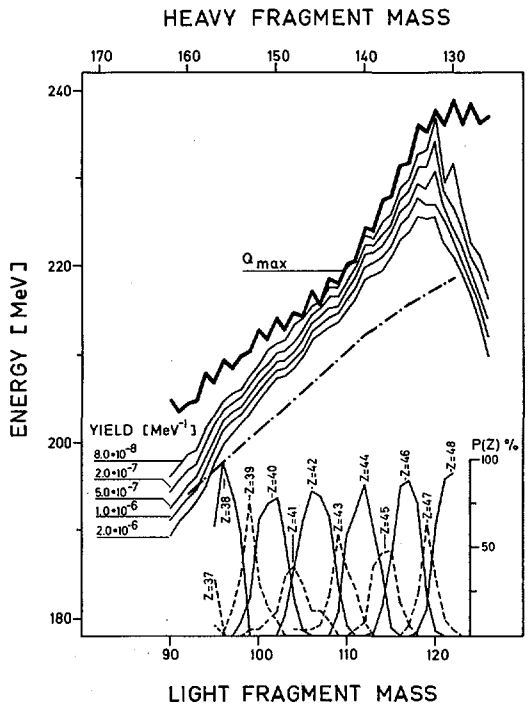

Fig. 9. Total kinetic energy versus light fission fragment mass at low yield levels and charge yields versus mass at TKE(A) ≥ TKE (A) + 27 MeV

figure shows the independent fractional charge yields $P(Z_L)$ as function of A_L. Yields belonging to even charge splits are connected with full lines whereas odd splits are connected with dashed lines. The structures of the TKE lines are clearly in phase with the even charge yields, showing that the TKE is relatively higher for even splits than for odd ones. Nuclei with even charge may be less deformable and be characterized by a more compact scission configuration. From the charge yield in Fig. 9, it can also be seen that even charge splits are 2-3 times more probable than odd splits in this TKE range. This suggests that the nuclear charge split is determined at an early stage of the fission process where the internal excitation of the fissioning system is so low that breaking of proton pairs is unlikely. On the contrary, neutron pairing is generally not conserved in cold fragmentation. Only for the lowest yield levels ($\sim 10^{-7}$ MeV^{-1}) does the TKE line partly reproduce the neutron even-odd effects as given by the Q_{max} line. At these low yield levels the "true" cold fragmentation limit may be reached where fragments are born without internal excitation. For fragmentation with lower TKE the neutron number seems then to be determined at a stage where the internal excitation energy of the fissioning system is so high that one or more neutron pairs are broken.

1.1.2 Non-Neutron Data for Standards

Half Life of ^{133}Ba

H.H. Hansen, D. Mouchel, R. Vaninbroukx, W. Zehner

The nuclide ^{133}Ba plays a significant rôle as an ^{131}I mock-up and as a multi-γ-ray reference source. The reliability of its application to detector efficiency calibration depends strongly on the accurate knowledge of the nuclide's half life. At CBNM the decay of this nuclide was followed for several years.

Three sources were made in 1974 from a standardized solution obtained from LMRI, Saclay. The amount of impurities in 1974 was given by the supplier to be less than 0.1 % of the ^{133}Ba activity. This limit of impurity concentration has been verified at CBNM by Ge(Li) and Si(Li) photon spectrometry. Two other sources were prepared in 1976 from a solution provided by TRC, Amersham. Impurity checks done at CBNM revealed γ-ray emitting contaminants at an upper limit of 0.1% relative to the ^{133}Ba activity at the time the half-life measurements were started.

Photon countrates have been recorded repeatedly using three detectors : a 7.5 cm × 7.5 cm NaI(Tl), a 18 cm^3 Ge(Li) and a 65 cm^3 pure Ge. Two different methods of photon registration have been applied : integral counting with the NaI(Tl) crystal and differential counting upon individual γ-ray lines with the solid-state detectors.

For all series of measurements the periods of observation have been subdivided into two halves and values for the half lives have been calculated within these sub-periods. No striking differences were found which would indicate time-dependent systematic effects. A weighted mean has been calculated to give the final result of 3838 days with an overall uncertainty of ± 12 days. Considering a mean number of 365.242 days per year the half life of ^{133}Ba is $T_{\frac{1}{2}}$ = (10.51 ± 0.03) a, which is in good agreement with values reported recently in the literature.

Alpha-Particle Emission Probabilities P_α of ^{237}Np

G. Bortels, D. Mouchel

The decay scheme of ^{237}Np is complex and not well known. In particular, the α-particle emission probability, P_α ,of the major transition feeding the 86.5 keV level in ^{233}Pa is presently known to only about 20%. The accu-

racy required for neptunium-mass determination in relation with the reactor fuel cycle is 1%.[1]

A measurement programme for P_α of ^{237}Np was started at CBNM in collaboration with AERE, Harwell and CIEMAT JEN, Madrid.

Sources of ^{237}Np on various substrate materials were produced at CBNM. Mixed ^{237}Np + ^{240}Pu sources were made on glass discs at AERE, Harwell.

Using one of these sources two series of about 150 spectra of three hours measuring time each were recorded with a 50 mm^2 ion-implanted detector in a solid angle of 1%. A new measurement chamber had been constructed with which peak broadening, resulting from drift in long-term measurements, is substantially reduced. The position of the major peaks for both the ^{237}Np and the ^{240}Pu part of the spectrum has been deduced for all spectra. It is shown that, apart from initial drift, the peak positions remain within one channel (0.66 keV) over a period of 2 weeks (Fig. 10). The spectrum shown in Fig. 11 was obtained by adding 119 spectra. The peak resolution for that spectrum is 9.7 keV at FWHM.

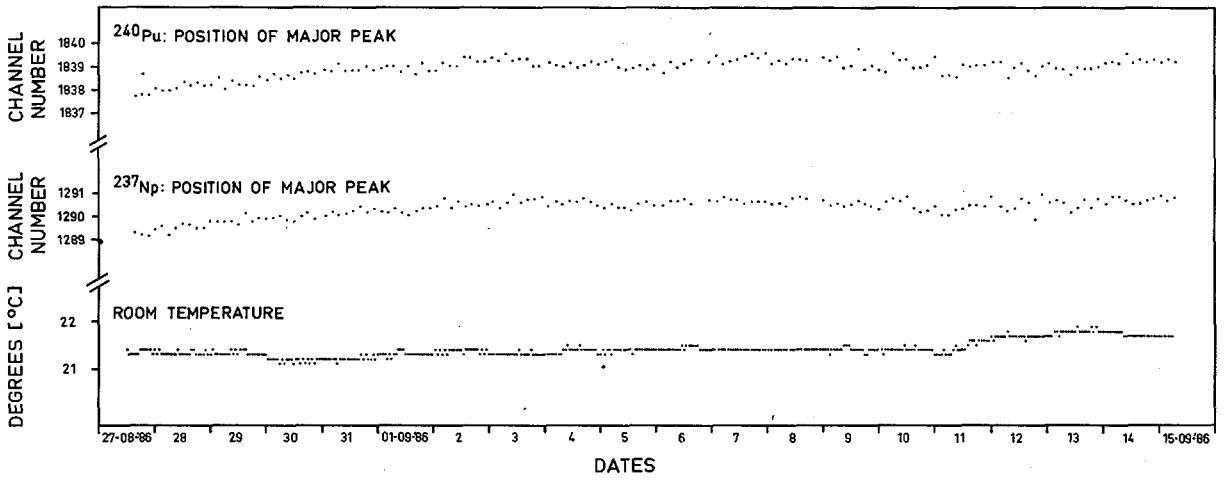

Fig. 10. Stability of peak position in successive alpha-spectrometric measurements of a mixed $^{237}Np/^{240}Pu$ source

This spectrum was analysed using an analytical function for the single peak which is the convolution of a Gaussian and a weighted sum of two exponentials. Thirteen peaks were fitted which provided a set of preliminary results for P_α. The spectrum of Fig. 11 was also analysed at CIEMAT JEN, Madrid, where the preliminary results have been discussed at the ICRM Workshop meeting on "Computer Analysis of Complex α-Particle Spectra", November 1986.

---

(1) Decay Data of Transactinium Nuclides, Technical Report Series N° 261 IAEA, Vienna (1986), p. 7

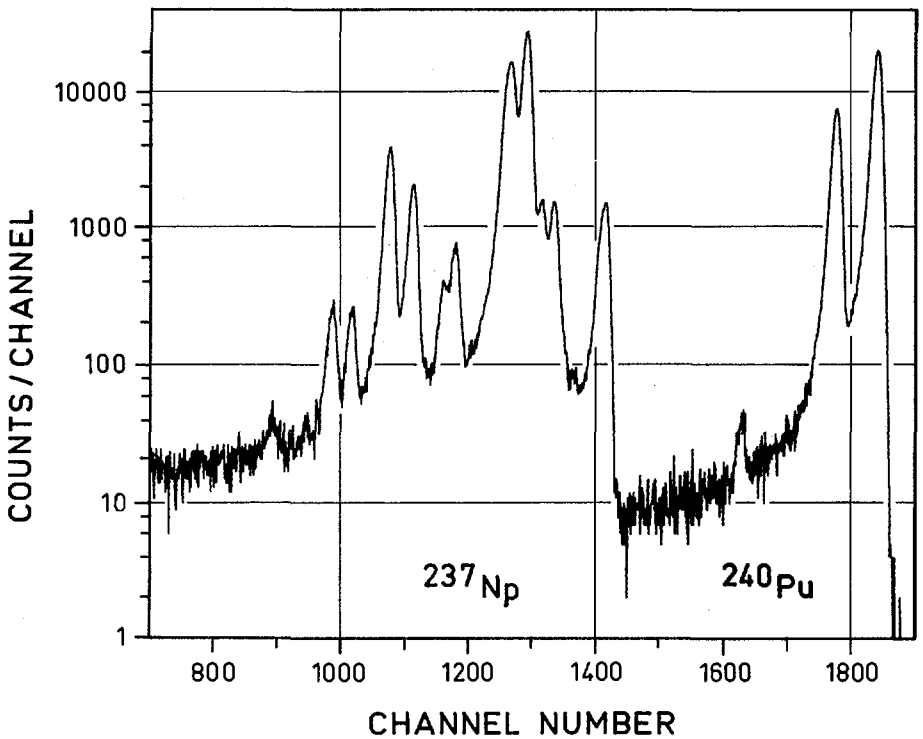

Fig. 11. Alpha-particle spectrum of a mixed $^{237}Np/^{240}Pu$ source

Decay of ^{241}Am

B. Denecke

The radionuclide ^{241}Am is widely used as γ-ray source for the efficiency calibration of photon spectrometers. According to the IAEA evaluations the accuracy of the emission probability of the 59.54 keV γ rays is still not better than 1% and the requirement of 0.2% is not yet fulfilled[1]. To deduce the γ-ray emission probability both the disintegration rate N_0 and the γ-ray emission rate $N_\gamma(60)$ have to be determined. Ten sources of various activities (80 Bq to 20 kBq) had been prepared by evaporation of ^{241}Am under vacuum onto 450 µg/cm^2 thick mylar foils. The purity of the sources was checked by α-particle spectrometry.

The disintegration rates N_0 of the sources were determined by counting the emitted α particles with an ion-implanted Si detector (diameter 61 mm). The solid angle for detection, defined by a carefully grounded diaphragm, was (0.3175 ± 0.0002) sr. In total 17 measurements were done. The accuracy reached is better than 0.15%.

(1) Decay Data of Transactinium Nuclides Technical Report Series N° 261, IAEA, Vienna (1986), p. 9

The γ-ray emission rates N_γ were measured with a 4π-CsI(Tl)-sandwich spectrometer. It consists of two CsI(Tl)-scintillation crystals of 5 cm in diameter and 2.4 cm thickness each of them with a semi-spherical cavity. The source is positioned in the center of the spherical cavity sandwiched between the crystals. The solid angle for detection of the 60 keV γ rays is 99.96% of 4π sr. Since the detectors are essentially windowless the α particles in the decay of ^{241}Am which are coincident with the 60 keV γ rays have to be stopped by absorbers, shaped like bowler hats as shown in Fig. 12. These absorbers were prepared with various thicknesses by hot pressing of high-density polyethylene.

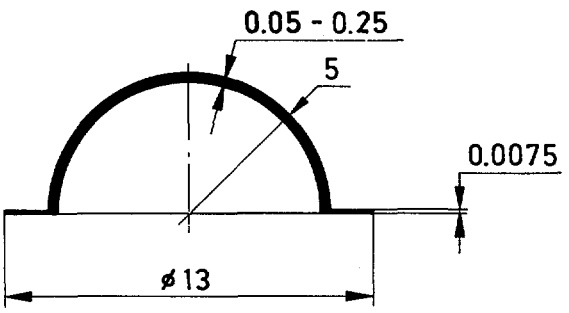

Fig. 12. Bowler-hat shaped polyethylene absorber to stop the α particles. Dimensions are given in mm

As a consequence of the spherical symmetry and the small size of these absorbers, the probability for absorption of secondary X rays and escape of photoelectrons or Compton electrons from the sensitive volume of the detectors is very small. No iodine- or cesium-escape peak nor other low-energy tailing were observed in the photonspectra. Only minor corrections for photon absorption and low energy tail discrimination have to be applied.

The total efficiency of the detection system was calculated by a Monte Carlo method which took into account the absorption in the backing foil, the hydrogen-filled gaps between foil and absorbers, the plastic absorbers and a possible transmission through the detectors.

Fig. 13 shows the photon-detection efficiency of the spectrometer for two absorbers of different thickness. The absorption of the 60 keV γ rays in the backing foil and the 8 mg/cm^2 thick α-particle absorbers is only (0.16 ± 0.03) %. A major source of uncertainty is due to coincidence summing of the various LX rays with the 26 keV γ rays and with the LX rays of coincident transitions from other levels. The impact of this effect on the spectrum decomposition is still under investigation.

Twenty γ-ray measurements were made with 7 sources. The reproducibility of the results is 0.1%.

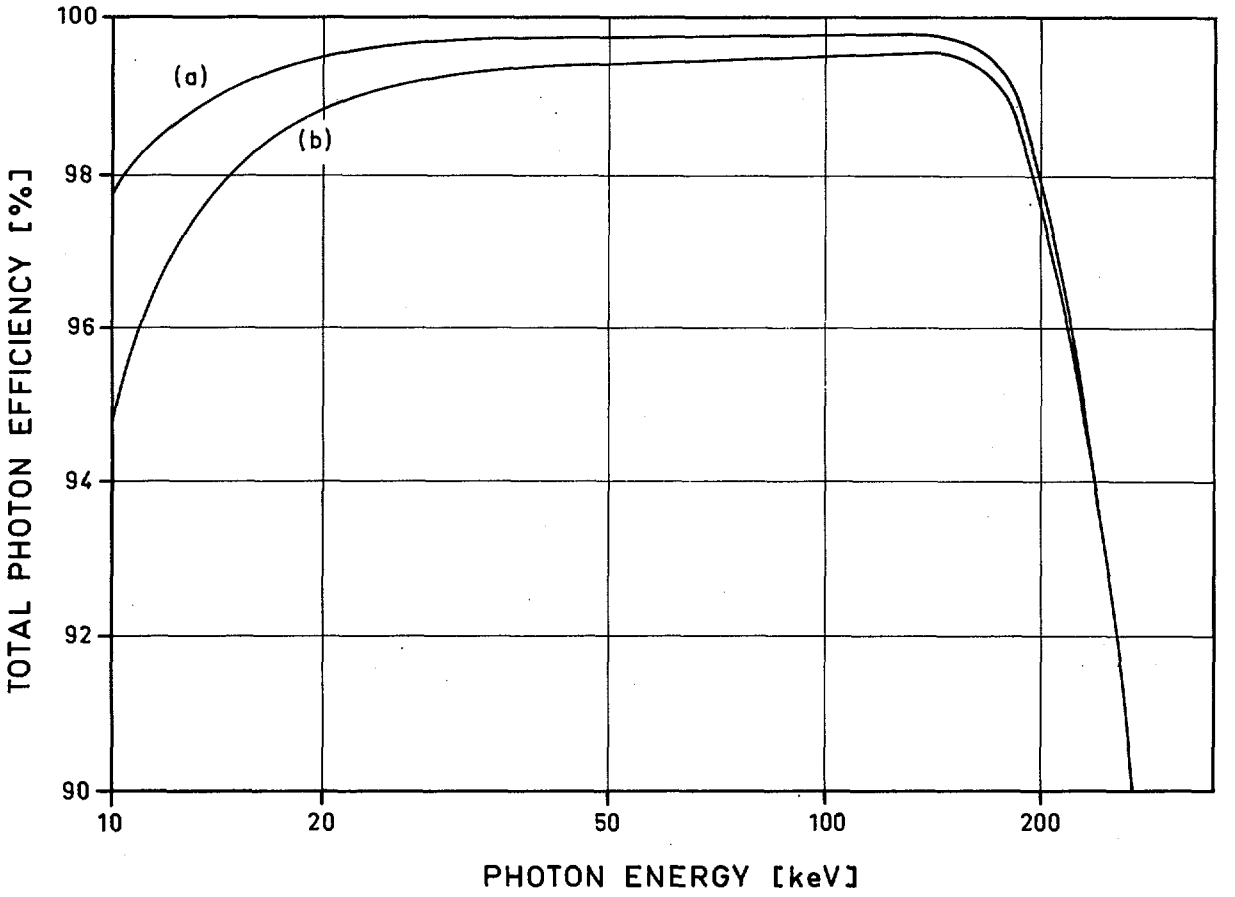

Fig. 13. Photon-detection efficiency of the 4π-CsI(Tl) sandwich spectrometer for two absorber thicknesses. Curve (a) for 8.3 and (b) for 23 mg/cm^2 absorbers of polyethylene

1.2 NUCLEAR DATA FOR FISSION TECHNOLOGY

In the field of nuclear data for fission technology the effort was concentrated on three subjects described in detail below: measurements of actinide data in the subthermal neutron energy range, a measurement of the fission cross section of ^{243}Am and measurements in connection with the NEANDC task force on the 1.15 keV resonance in ^{56}Fe. Besides these main items, work continued on the analysis of total and radiative capture cross-sections of the chromium isotopes. Similar measurements have been started on nickel isotopes.

1.2.1 Neutron Data of Actinides

Fission Cross-Section Measurements at Very Low Energies

C. Wagemans*, A. Deruytter, R. Barthélémy, J. Van Gils*
(European High Priority List NEACRP-A-568, NEANDC-A-180)

In order to reduce the uncertainty on the cross-section data in the subthermal region, a series of measurements of the $^{235}U(n,f)$ cross section has been performed down to 1 meV neutron energy. In two measurements, the $^{6}Li(n,\alpha)T$ reaction has been used as a neutron flux monitor. In a third measurement the $^{10}B(n,\alpha)^{7}Li$ reaction has been used, and in a fourth control measurement, the $^{6}Li(n,\alpha)T/^{10}B(n,\alpha)^{7}Li$ ratio has been determined to make sure that the neutron flux monitor has no impact on the $\sigma_f(E)$ value.
With the same experimental facility, also the $^{239}Pu(n,f)$ cross section has been measured relative to $^{6}Li(n,\alpha)T$. All these measurements are being analysed simultaneously.

Eta, η, of ^{235}U

H. Weigmann, J.A. Wartena, C. Bürkholz
(WRENDA 83/84 request N° 465 and European High Priority List NEACRP-A-568, NEANDC-A-180)

A first series of measurements of the energy dependence of eta of ^{235}U have been described in the preceding progress report.[1] In that report also the difficulties associated with beam-dependent backgrounds are described. In order to further investigate these background effects, a supplementary mea-

---

* SCK/CEN, Mol, Belgium
[1] NEANDC (E) 272 "U" Vol. III Euratom; INDC (EUR) 020/G (1986), p.25

surement series has been performed, where the originally 2 cm thick beryllium filter was replaced by one of 6 cm thickness. Since the available filter had a diameter of only 4 cm, the collimation of the neutron beam had to be reduced correspondingly. Thus, the reduction of the beam-dependent background at low neutron energies was accompanied by a reduction of the useful flux, i.e. a relative increase of the beam-independent background and increase of the statistical uncertainty.
The results of these measurements, although less accurate, are in full agreement with the data reported earlier [1], i.e. with a constant value of eta for sub-thermal energies. The fact that this agreement is obtained with strongly changed conditions with respect to the beam-dependent background, gives additional confidence to the background treatment in the earlier measurements.

Fission-Fragment Mass and Energy Distributions for the Spontaneous Fission of the Plutonium Isotopes

C. Wagemans*, P. Schillebeeckx*, A. Deruytter, R. Barthélémy

In the frame of a systematic investigation of the fission-fragment mass and energy distributions of the plutonium isotopes, most of the spontaneously fissioning $^{238,240,242}Pu$ isotopes have already been studied previously relative to the $^{239}Pu(n_{th}, f)$ reaction. For these isotopes, strong neutron shell effects were observed, which appeared to be very enhanced when a closed shell occured in both the light and the heavy fission fragment. It is expected that the probability for such combinations be particularly high for ^{236}Pu. Thus, a measurement of the spontaneous fission reaction of that plutonium isotope has been started.

^{243}Am Fission Cross-Section Measurements

H.-H. Knitter, C. Budtz-Jørgensen
(WRENDA request N°s 712111 R, 792236 R)

The nuclide ^{243}Am is produced in nuclear power reactors as an unwanted by-product. The rate by which it is produced in a 1200 MW power station lies between a few $kg \cdot a^{-1}$ and 75 $kg \cdot a^{-1}$, depending on the reactor type and fuel composition. After a cooling time of ten years for burnt fuel elements

---

* SCK/CEN, Mol Belgium
(1) NEANDC (E) 272 "U" Vol. III Euratom; INDC (EUR) 020/G (1986), p. 25

the abundance of ^{243}Am among the minor transactinium isotopes is between 15 % and 50%. Therefore ^{243}Am is a rather important constituent of radioactive material in burnt fuel. The present data base of the minor actinides is sufficient for the prediction of the production rate, but insufficient for the study of new concepts for their incineration. In particular, the knowledge of the ^{243}Am fission cross section is very unsatisfactory and corresponding measurements in the range from thermal to 15 keV are requested yielding results with an accuracy of better than 15 %. The fission cross section of ^{243}Am was measured with an ionization chamber in a back-to-back geometry relative to the ^{235}U standard fission cross section, using the 7 MV Van de Graaff accelerator and GELINA as pulsed neutron sources.

At the Van de Graaff quasi-monoenergetic neutrons were produced covering a neutron energy range from 0.33 to 10 MeV. With the Van de Graaff being operated in pulsed mode, the conventional time-of-flight technique was employed to measure simultaneously with the prompt fission events also the time-uncorrelated background, which in all measurements was less than 0.6 %.

At the GELINA moderated and pulsed white neutron source the fission chamber was exposed to a neutron beam at a neutron flight-path length of 8.392 m. The accelerator was operated with a pulse width of 4 ns, a repetition rate of 800 Hz, and an average electron-beam power of 10 kW at 100 MeV. A cadmium cut-off filter (1 mm thick) was used to remove neutrons with flight times longer than the time between two successive bursts. The neutron energy spectrum extended therefore from about 1 eV to several MeV. Since below 30 keV neutron energy the $^{235}U(n,f)$ standard cross section shows considerable structure, an additional measurement of the neutron flux shape was performed with an ionization chamber loaded with ^{6}LiF.

In Fig. 14 the present results for neutron energies up to 10 MeV are shown together with data from earlier measurements and evaluated files. Fig. 15 shows the present results for neutron energies down to 100 eV. Between 100 eV and 10 keV no reliable fission cross section data existed and therefore the present data add entirely new information to the data base. In the absence of experimental data the three recent evaluated files JEF-1, JENDL-2 and ENDF/B-5 fail in their prediction by factors between 2 and even larger than 10 in this, for reactors important, energy range. Below 1 keV neutron energy the fission cross section shows pronounced structure. The fission areas of 31 isolated resonances below 56 eV have been determined.

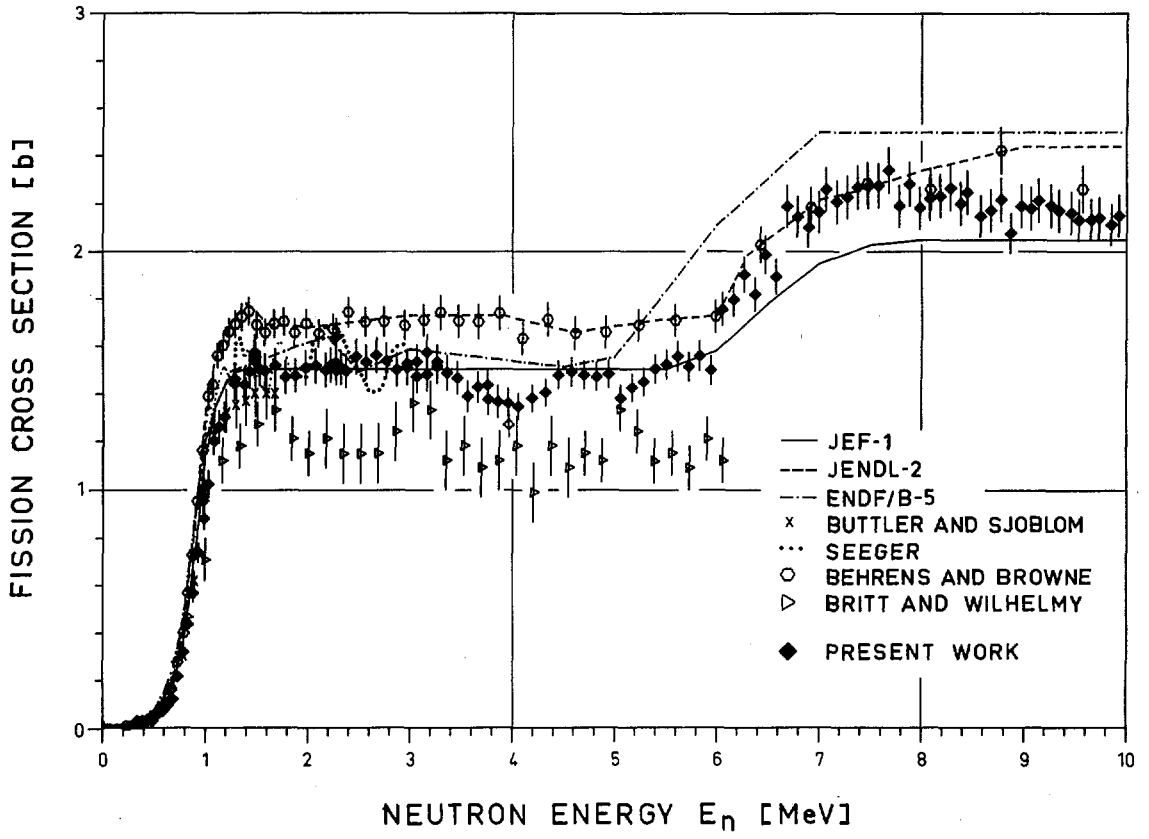

Fig. 14. The ^{243}Am(n,f) cross section in the MeV energy region

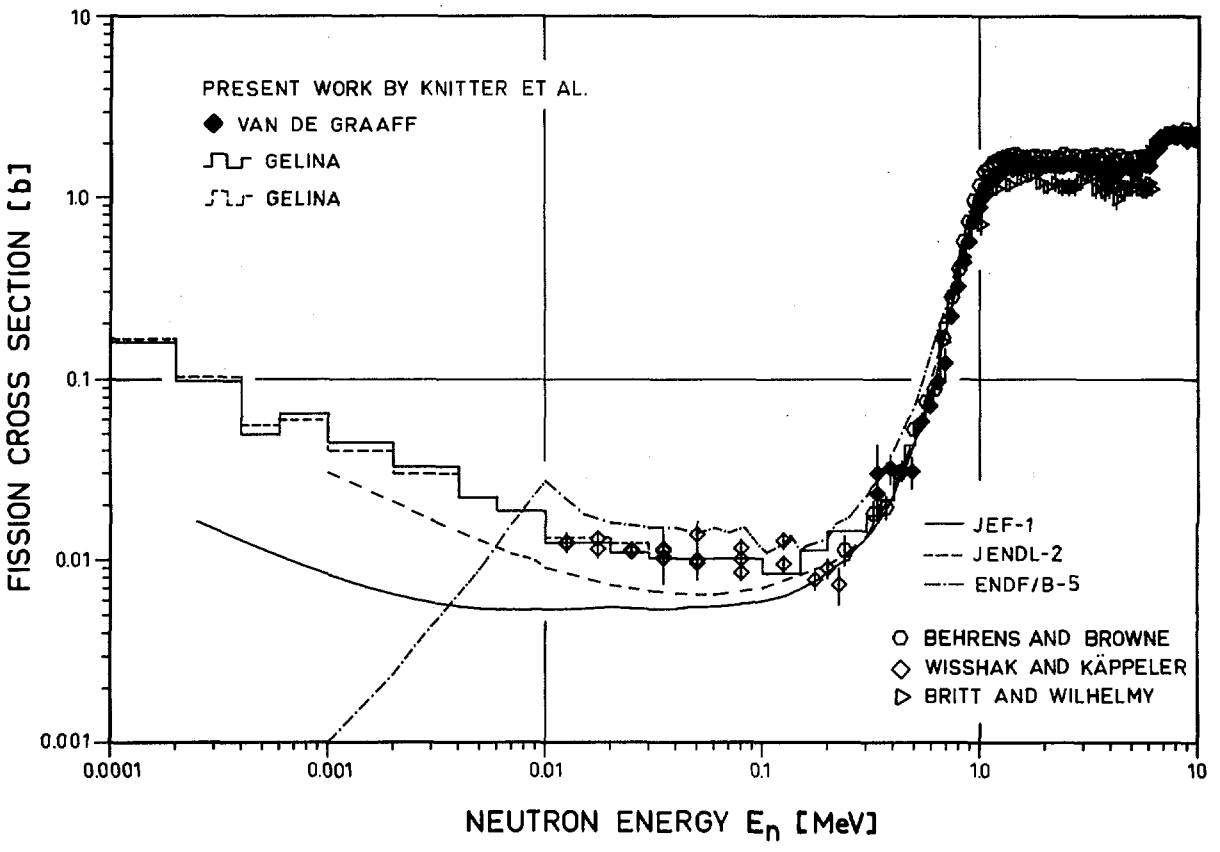

Fig. 15. The ^{243}Am(n,f) cross section between 100 eV and 10 MeV neutron energy

1.2.2 Neutron Data of Structural Materials

Experimental Determination of the Weighting Function of a C_6D_6 Detector

F. Corvi, A Prevignano*, P.B. Smith**, H. Liskien, F. Gasperini
(relevant to 1.15 keV ^{56}Fe Task Force of NEANDC)

The response functions and the efficiencies of a cylindrical C_6D_6 liquid scintillator were measured at the 7 MV Van de Graaff for a number of γ-ray energies in the range 0.5-10 MeV. The method devised consists of measuring transitions from (p,γ) resonance reactions both in single mode and in coincidence with signals from a coaxial Ge detector. When capture proceeds through a few strong two-step cascades, as it is often the case in resonances of light nuclei, the C_6D_6 efficiency for one γ ray can be derived via the coincidence method, i.e. by determining the ratio between the peak areas of the complementary γ ray in the coincident and single Ge spectra, respectively. Similarly, the response function of a given γ ray is obtained from those C_6D_6 pulses which are in coincidence with the full peak of the complementary transition.
Targets of ^{26}Mg have been used at proton energies of 1001 and 2220 keV, of ^{30}Si at 1398 keV and of ^{34}S at 1211 keV. The raw data must be corrected for two effects: 1) interference from 3- or 4-step cascades going through the same intermediate state as the 2-step cascade under consideration and 2) angular correlation effects. A correction for the first effect was calculated from the known data of the decay schemes of the investigated resonances. In the case of the ^{26}Mg target, the results were checked with an independent measurement of NaI(Tl)-Ge coincidences. In general, more cascades were discovered than reported in the literature. The second effect was minimized by placing the axis of the Ge crystal at Θ = 0° and that of the C_6D_6 detector at Θ = 125° with respect to the proton beam direction. This choice eliminates the contribution of the second order Legendre polynomial $P_2(\cos\Theta)$, which is usually the dominant one. A computer programme was written which calculates (p,$\gamma\gamma$) angular corrections starting from the knowledge of the proton orbital angular momentum, the spins of all states involved and the quadrupole-to-dipole mixing ratios of the γ rays. It was found, that, for the cases investigated, the correction for angular correlation is always negligible. The results were checked

---

* EC Fellow
** University of Groningen, Groningen, The Netherlands

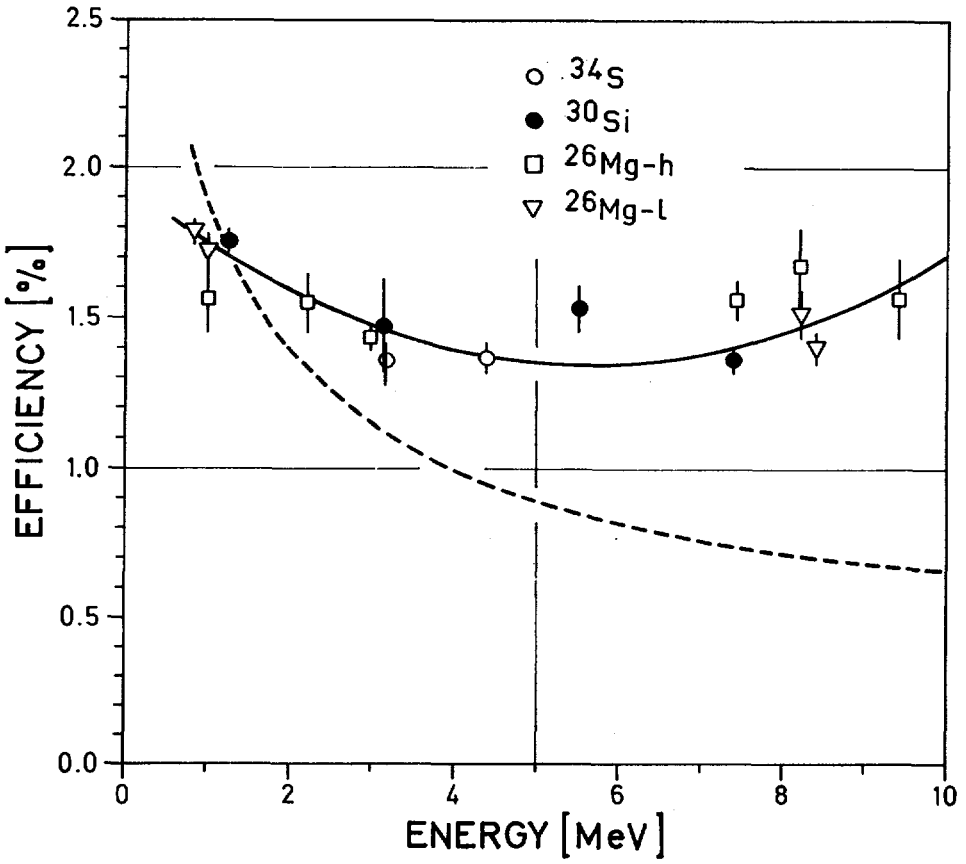

Fig. 16. Experimental values of the absolute efficiency of the C_6D_6 detector plotted vs γ-ray energy. The solid line is a parabolic fit to the data while the dotted line is a result of calculations

with a series of NaI(Tl)-Ge correlation measurements: the experimental correction coefficients were found to be unity, within the errors. The absolute efficiency values of a C_6D_6 scintillator of 10.2 cm diameter and 7.6 cm height placed at 7.6 cm from the target, are plotted for 16 γ rays in Fig. 16: the full line is a parabolic fit to the data while the dotted line represents the efficiency calculated according to the "any interaction" hypothesis. This simply assumes a detection probability $\varepsilon = 1-\exp(-\mu \cdot d)$ for a γ ray having a path of length d in the detector and a total linear attenuation coefficient μ. Although it is a rather crude approximation, this curve is quite adequate to evidence the most conspicuous result of the present investigation: the measured efficiency in the range 0.5-10 MeV does not decrease with energy as foreseen by any kind of calculation but stays rather constant. This result is not understood. In Figs. 17a and 17b are plotted the unnormalized response functions for 12 transitions below 9 MeV. These data were used to compute the weighting function (WF) approximated by a 4th degree polynomial going

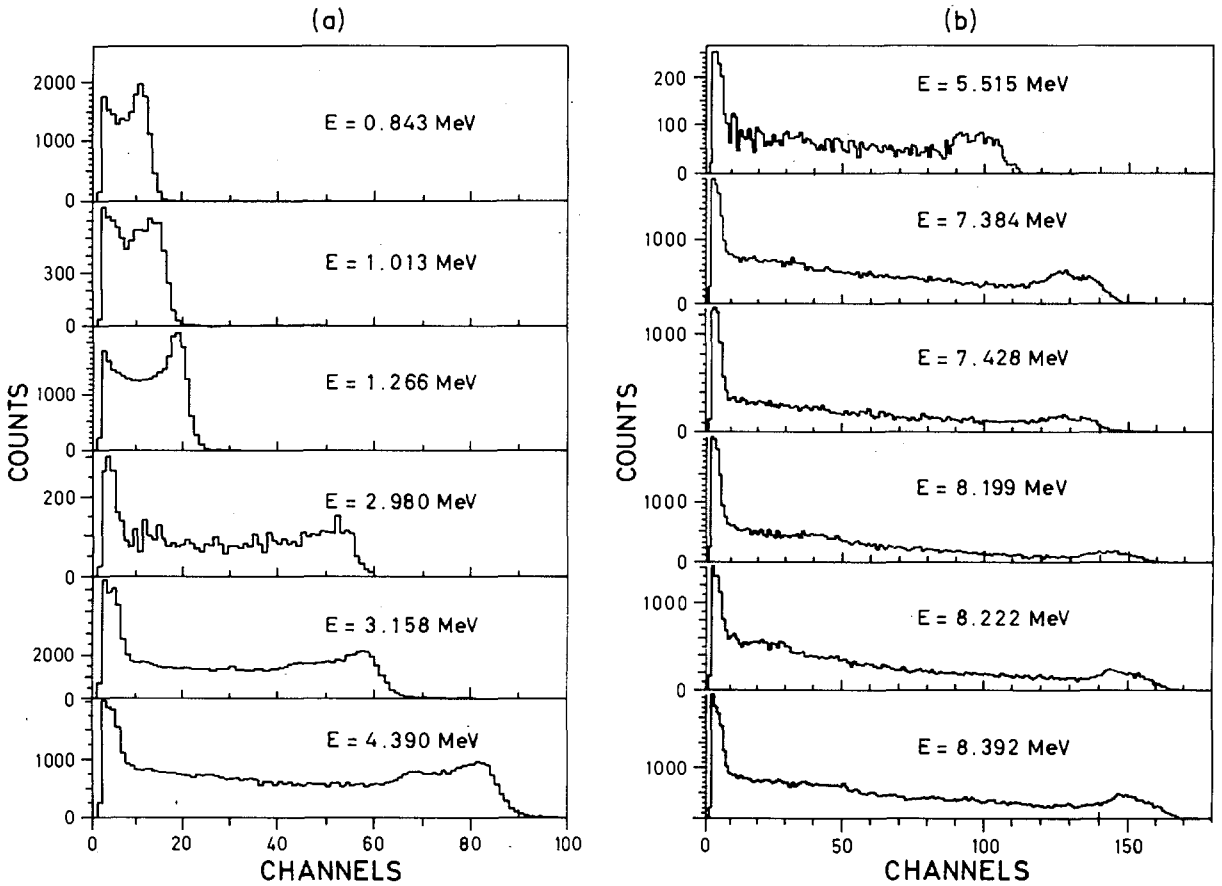

Fig. 17. Response function for 12 γ rays; energy E from (a) 0.843 to 4.390 MeV and (b) 5.515 to 8.392 MeV. Energy calibration is 50 keV/channel. Note: scaling of abscissae and ordinates is different in (a) and (b)

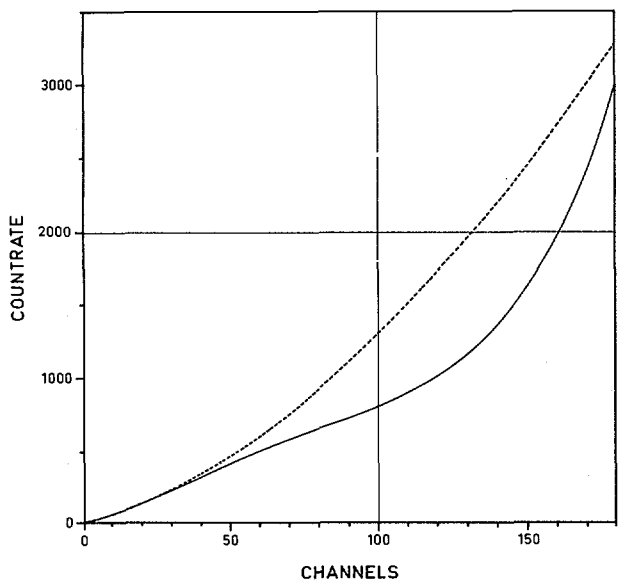

Fig. 18. "Experimental" (full line) and "calculated" (dashed line) weighting function: the two curves are normalized to the same value at channel 20

through the origin. The "experimental" WF is plotted in Fig. 18 (full line) together with the WF derived from Monte Carlo simulation of the detection process (dotted line) and used up to now in neutron capture.

Finally, the parameters of the 1.15 keV ^{56}Fe resonance have been recalculated by applying the experimental WF derived above to the original data from 1982[1]. By normalizing the data to the 5.2 eV saturated resonance of silver we obtain $A_\gamma = g\Gamma_n\Gamma_\gamma/\Gamma = (54.9 \pm 2.3)$

(1) F. Corvi et al., Proc. Int. Conf. on Nuclear Data for Science and Technology, Antwerp (1982), p. 131

meV compared to the value A_γ = 67.3 meV obtained with the calculated WF. The error includes an estimated 3.4 % due to the WF shape. The new value is in excellent agreement with that of A_γ = (55.7 ± 0.8) meV derived from the ORNL transmission measurements[1].

To conclude: the present exercise has been successful in predicting a weighting function which reconciles capture and transmission data. However, more work is needed in order to find a plausible explanation for the data plotted in Fig. 16.

1.2.3 Matters Related to Fission Technology

Investigation of an Optimized 24 keV Neutron Beam Filter.

A. Brusegan, C. Van der Vorst
(Request from GKSS, Geesthacht)

In their recent review article, Block and Brugger[2] point out that strong quasi-monoenergetic neutron sources delivering a continuous beam are increasingly being applied in the fields of neutron physics, health physics, dosimetry and radiobiology. The authors make detailed proposals concerning the use of filters, most of which require a good knowledge of the quasi-monoenergetic beam-intensity distribution and the amount of high-energy neutrons still present in the beam. The reason for this unwanted contribution is the presence of other windows in the transmission of the filter material. Their effect may be considerably reduced by using additional suitably selected materials for the filter, which do not affect the main, but screen the other windows.

In the investigated case of the 24 keV window, an iron filter stack composed of 350 mm of iron, 230 mm of aluminium and 75 mm of cast sulfur has been used. Following a procedure quoted by Kuzin et al.[3], titanium has been applied as an additional filter material to determine the intensity of neutrons with energies E > 24 keV by the "filter-difference" method: 5 mm of titanium screen the predominant 24 keV line, but leave the high-energy part of the neutron spectrum almost unchanged.

---

(1) F.G. Perez, J.A. Harvey and N.W. Hill, private communication to NEANDC Task Force (1986)

(2) R.C. Block and R.M. Brugger, Filtered Neutron Beams, in Neutron Physics and Nuclear Data in Science and Technology, (S. Cierjacks, ed.), "Neutron Sources for Basic Physics and Applications" Pergamon Press, Vol. 2 (1983), p. 177

(3) E.N. Kuzin et al., Spectra of Filtered Neutron Beams from the Obninsk Reactor , Sov. Atom. Energy 35 (1973) 1089

At the neutron total-cross-section facility of GELINA the spectral distribution of the neutrons transmitted through that composite filter* has been studied. The accelerator was running with a repetition frequency of 800 Hz and an electron-burst width of 1 ns. The neutrons were detected at 98.24 m flight distance by a 0.5 cm thick sintered B_4C slab (92% enriched in ^{10}B) viewed by four 10 cm x 7.5 cm NaI(Tl) scintillators. The complete set-up was screened with lead and borated paraffin.

In the present experiment the samples were so thick that the variations in neutron-beam intensity from the "sample in" to the "sample out" position caused gain variations of the phototubes. Photons of a ^{133}Ba γ ray source ($E_\gamma \leq 384$ keV) placed in the vicinity of the scintillators were used to stabilize the gain of the phototubes via a suitable electronic device. The following experiments have been performed using a 4 position sample changer: a) composed iron filter stack + titanium sample in the beam, b) composed iron filter stack in the beam, c) "Open" beam, and d) sodium + sulfur + silicon black resonance filters in the beam.

From runs a), b) and c) the transmission of the "Fe + Ti" stack and that of the "Fe" stack alone could be obtained, run d) served for the background determination of the open beam run c).

In order to investigate the beam dependent background contributions, the background measurements have been repeated, replacing the ^{10}B slab by a 0.62 cm thick carbon sample (measured density = 1.6 g/cm^3).

In the energy range from 1 keV up to 650 keV, the deviations of the final transmission spectra due to the two different background determinations were on the average 2%, which is assumed to be a measure of the systematic error.

In Table 1, some average properties of the "difference" of the "Fe" stack and of the "Fe + Ti" stack transmission spectra are given. Averages are calculated by taking the measured transmission points as weighting quantities. The quoted standard deviations include statistical errors only. Plots at 24 keV are given in Fig. 19, a, b and c for the "difference", the "Fe" stack and the "Fe + Ti" stack transmission spectra, respectively.

---

* Supplied by Dr. H.G. Priesmeyer, Institut für Reine und Angewandte Kernphysik der Christian Albrecht Universität, Kiel, and GKSS, Geesthacht, Germany

Table 1. Some average properties of various transmission spectra

	DIFFERENCE SPECTRUM	Fe-STACK SPECTRUM	Fe + Ti STACK SPECTRUM
ENERGY RANGE [keV]	18.40 - 25.92	18.40 - 25.92	18.40 - 25.92
AVER.ENERGY [keV]	23.903	23.968	24.130
ERROR [keV]	0.0051	0.0032	0.0067
STAND.DEV [keV]	0.9969	0.9931	0.9639
AVERAGE TRANSM	0.018890	0.026233	0.007342
ERROR	0.000072	0.000068	0.000035
ENERGY RANGE [keV]	66.96 - 71.47	66.96 - 71.47	66.96 - 71.47
AVER.ENERGY [keV]	69.11	69.76	69.93
ERROR [keV]	0.546	0.082	0.11
STAND.DEV.[keV]	0.9795	1.020	0.960
AVERAGE TRANSM	0.000082	0.000391	0.000309
ERROR	0.000035	0.000025	0.000024
ENERGY RANGE [keV]	72.6 - 73.4	72.6 - 73.4	72.6 - 73.4
AVER.ENERGY [keV]		72.98	73.05
ERROR [keV]		0.033	0.040
STAND.DEV.[keV]		0.213	0.189
AVERAGE TRANS.	0.000040	0.000443	0.000404
ERROR	0.000088	0.000063	0.000062
ENERGY RANGE [keV]	125.6 - 129.3	125.6 - 129.3	125.6 - 129.3
AVER.ENERGY [keV]		128.14	128.13
ERROR [keV]		0.027	0.027
STAND.DEV.[keV]		0.778	0.773
AVERAGE TRANSM.	0.000039	0.001976	0.001937
ERROR	0.000075	0.000053	0.000053
ENERGY RANGE [keV]	179.3 - 187.3	179.3 - 187.3	179.3 - 187.3
AVER.ENERGY [keV]		183.51	183.62
ERROR [keV]		0.42	0.44
STAND.DEV.[keV]		2.029	1.077
AVERAGE TRANSM	0.000007	0.000118	0.000112
ERROR	0.000030	0.000021	0.000022
ENERGY RANGE [keV]	242.4 - 245.1	242.4 - 245.1	242.4 - 245.1
AVER.ENERGY [keV]		243.83	244.00
ERROR [keV		0.16	0.19
STAND.DEV.[keV]		0.667	0.455
AVERAGE TRANSM	0.000009	0.000225	0.000216
ERROR	0.000068	0.000048	0.000040

	DIFFERENCE SPECTRUM	Fe-STACK SPECTRUM	Fe + Ti STACK SPECTRUM
ENERGY RANGE [keV]	259.3 - 275.9	259.3 - 275.9	259.3 - 275.9
AVER.ENERGY [keV]		271.24	270.91
ERROR [keV]		0.11	0.12
STAND.DEV [keV]		3.349	3.396
AVERAGE TRANSM	0.000148	0.001266	0.001118
ERROR	0.000045	0.000032	0.000031
ENERGY RANGE [keV]	303.6 - 314.8	303.6 - 314.8	303.6 - 314.8
AVER.ENERGY [keV]		307.97	309.28
ERROR [keV]		0.64	0.62
STAND.DEV.[keV]		2.639	2.350
AVERAGE TRANSM	-0.000006	0.000115	0.000121
ERROR	0.000035	0.000024	0.000025
ENERGY RANGE [keV]	328.4 - 332.6	328.4 - 332.6	328.4 - 332.6
AVER.ENERGY [keV]		330.92	331.26
ERROR [keV]		0.31	0.61
STAND.DEV.[keV]		0.658	0.759
AVERAGE TRANS.	0.000082	0.000183	0.000101
ERROR	0.000059	0.000043	0.000041
ENERGY RANGE [keV]	339.7 - 361.2	339.7 - 361.2	339.7 - 361.2
AVER.ENERGY [keV]		352.29	352.53
ERROR [keV]		0.14	0.16
STAND.DEV.[keV]		3.593	3.460
AVERAGE TRANS.	0.000162	0.001078	0.000917
ERROR	0.000045	0.000033	0.000031
ENERGY RANGE [keV]	601.0 - 614.9	601.0 - 614.9	601.0 - 614.9
AVER.ENERGY [keV]		608.91	608.94
ERROR [keV]		0.27	0.29
STAND.DEV.[keV]		2.354	2.210
AVERAGE TRANSM.	0.00006	0.000928	0.000864
ERROR	0.00011	0.000077	0.000077

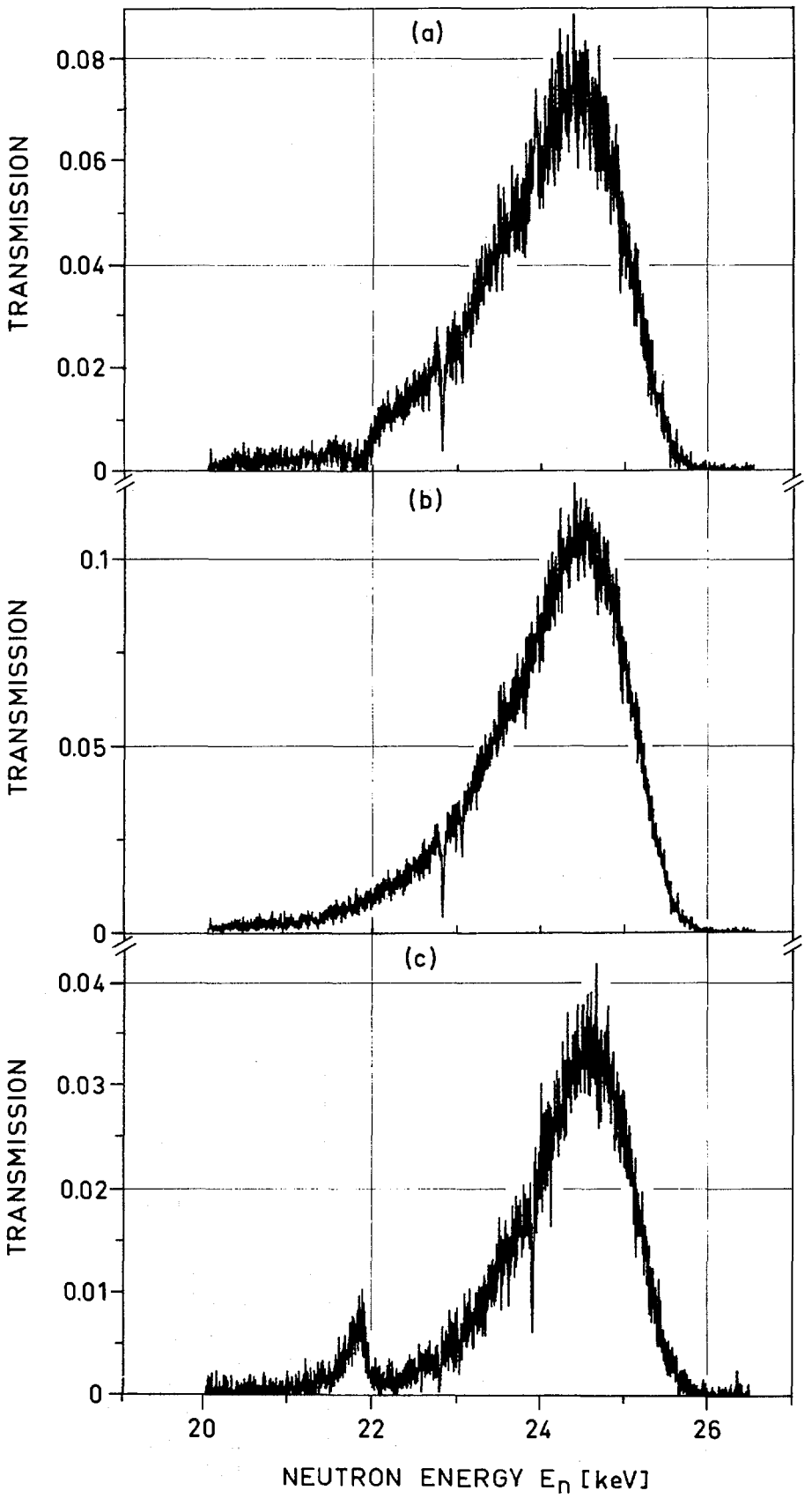

Fig. 19. Neutron transmission spectra for various filters or combination: (a) "difference" (b) "Fe" stack, (c) "Fe + Ti" stack

1.3 NUCLEAR DATA FOR FUSION TECHNOLOGY

Angular Distribution of Neutrons Scattered on ^{7}Li

H. Liskien, S. Bao*

Results on the angular distribution of neutrons inelastically scattered on the first excited state (Q = - 478 keV) of ^{7}Li as obtained by analyzing Doppler-broadened γ-ray lines were finalized for primary neutron energies between 4 and 8.5 MeV. Measurements had been made also at 9, 9.5 and 10 MeV. However, it turned out that those results could not be analyzed due to a too big correction for D(d,np) break-up neutrons. The results were presented at the International Conference on Fast Neutron Physics, Dubrovnik, May 1986.

A proposal has been worked out to include this information in the European Fusion File (EFF). Due to the poor data situation all evaluations (JEF-1, JENDL-2, JENDL-3) simply assume isotropy in the center-of-mass system. The only exception is the ENDF/B-5 evaluation which uses theoretical calculations: below 6 MeV an R-matrix result[1], above 8 MeV DWBA results[2] and a smooth connection between 6 and 8 MeV. However, the value of the R-matrix calculation is overestimated. The same authors have meanwhile published a second calculation with a different assumption on the ^{8}Li level scheme[3] and this yields very different results. The proposal shown in Fig. 20 assumes center-of-mass isotropy up to $E_n \approx 4$ MeV which is supported by earlier neutron experiments[4], uses the new

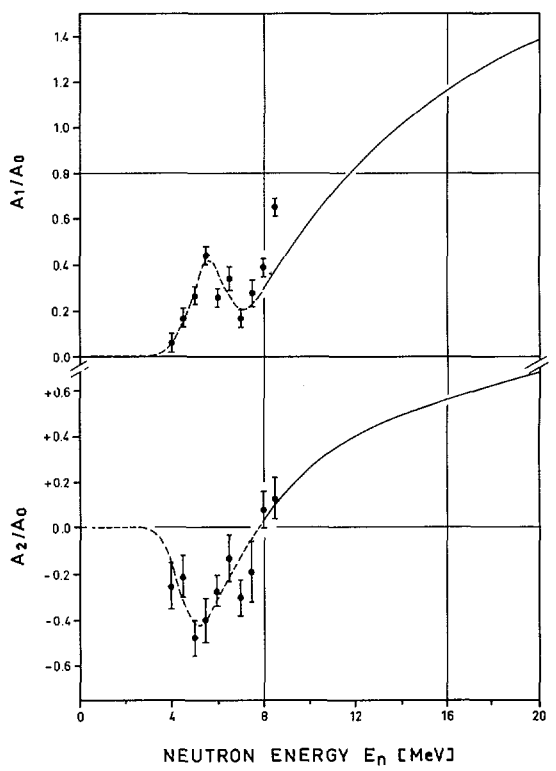

Fig. 20. Relative Legendre coefficients for the reaction ^{7}Li(n,n'$_1$)(Q = - 478 keV). The full line above 8 MeV stems from DWBA calculations. The dotted line assumes center-of-mass isotropy up to 4 MeV and the dots represent the present experimental data between 4 and 8 MeV

---

* Visiting Scientist from University Beijing, Beijing, PR of China

(1) H.D. Knox and R.O. Lane, Nucl. Phys. A359 (1981) 131

(2) P. Young, Private communication (1985)

(3) H.D. Knox, Radiation Effects 95 (1986)

(4) H.H. Knitter and M. Coppola, EUR 3903. e (1968)

data in the 4 to 8 MeV region and again the DWBA results above 8 MeV. This proposal has been translated into ENDF/B format.
A more general contribution "Neutron Angular Distribution from ^{7}Li" has been presented as invited review paper for the 2nd IAEA AGM on "Nuclear Data for Fusion Reactor Technology" in December 1986 at Gaussig/Dresden. It reports on the state of knowledge of angular distributions of all emitted neutrons after interaction of primary neutrons with the breeder material ^{7}Li. It develops a proposal to parameterize the neutron continuum in a more physical way by separating the elastic and inelastic components and by distinguishing between three-particle break-up and two-step consequential decay. This approach should lead to a better energy-angle correlation.

Double-Differential Neutron-Emission Cross Sections for ^{7}Li

E. Dekempeneer*, H. Liskien, L. Mewissen** and F. Poortmans**

Double-differential neutron-emission cross section data for the 1 to 16 MeV incident neutron energy range are requested for neutron transport calculations in the blanket of a fusion reactor. Materials which will most likely be used in significant quantities in the blanket are lithium as the tritium breeding material through the reactions ^{6}Li(n,α)T and ^{7}Li(n,n'α)T, beryllium or lead as neutron multipliers through the (n,2n) reactions, and the main structural materials iron and nickel. Measurements were started in which a pulsed white neutron source is used so that the cross sections can be obtained for all incident energies simultaneously. The first material studied is lithium. The experiment is built up at GELINA. The machine is operated at a repetition rate of 800 Hz with an average total beam power of 8 kW and an electron burst-width of less than 1 ns.
The scattering sample is positioned at 60 m from the neutron source. The incident neutron beam is collimated to a diameter of 5 cm. Samples are 7 cm diameter metallic ^{7}Li discs with an isotopic enrichment of 99.97 % (sample-thicknesses are 0.0324 and 0.0654 at/b). They are mounted in a 2.5 m long thin-walled aluminium vacuum tube to reduce air-scattering of the incoming neutrons and to prevent oxidation of the sample. The tube is placed parallel to the incident neutron beam. The secondary neutrons are detected with six NE 213 liquid scintillators surrounding the sample at a

* Visiting Scientist from the Free University of Brussels, Brussels, Belgium
** SCK/CEN, Mol, Belgium

distance of 20 cm. Pulse shape discrimination is applied to separate neutron from γ-ray events.
The incident neutron energy is determined by the time-of-flight method, in which the stop signal is derived from the detection of a secondary particle or γ ray. This method provides an accurate measure of the real flight time since the distance covered by the secondary particles (20 cm) is negligible compared to the flight-path length of the primary neutrons (60 m).
The secondary neutron energy is determined by unfolding the pulse-height distributions as observed in the scintillators. A paper on the principles of the method applied is in print in Nucl. Instr. Meth.
The results obtained with the two different samples agree well above 1.5 MeV secondary neutron energy. At lower energies systematic deviations, of about 10 % for the 'elastic' scattering data and up to 30 % for the non-elastic neutron-emission data, appear. These deviations are due to instabilities in the pulse shape discrimination over longer periods, which disturb the pulse-height spectra in the lower pulse-height region. The thick sample run yields the highest cross-section values, indicating that in this case probably a small γ-ray background is still present. For the 'elastic' scattering data the observed small deviations are taken into account in the uncertainty considerations. For the non-elastic double-differential neutron-emission cross sections a lower bias of 1.5 MeV secondary neutron energy was chosen. However, when determining the discrete scattering yields for the 4.63 and 6.54 MeV states there is no restriction to the use of this threshold. Indeed, since these yields are obtained after subtraction of an underlying continuum the data of the thick sample run can be used because in this case the probably existing γ-ray background will be subtracted as well.
The double-differential neutron-emission cross sections will be available from the neutron data centers through the EXFOR system. The 'elastic' and inelastic scattering data are discussed below.
The highest energy peak in the secondary neutron spectra, which is the sum of elastic and inelastic scattering to the first level of ^{7}Li, is well separated from the other non-elastic reaction channels and has been integrated. For comparison, data obtained from recent evaluations were first folded with the experimental incident energy bin-width and for the angular spread of our detector-system. The various evaluations deviate

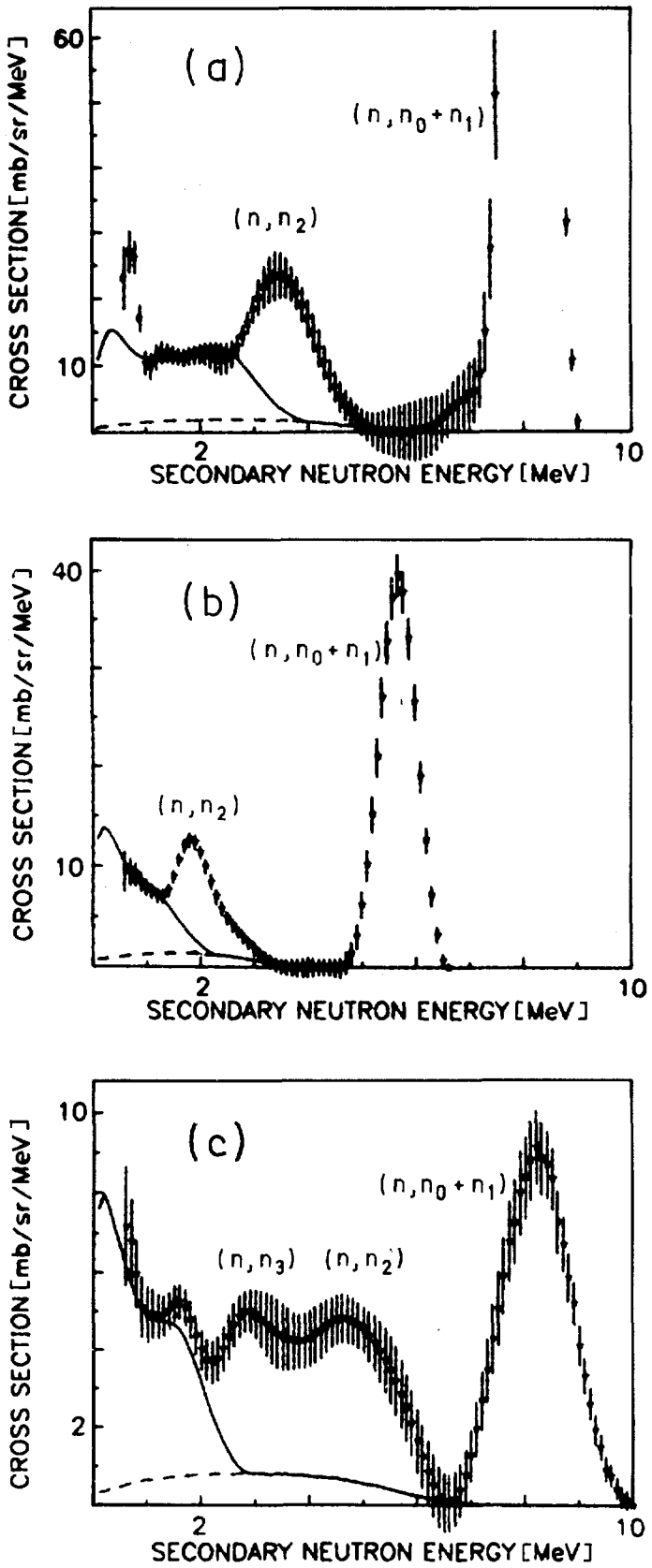

Fig. 21. Double-differential neutron-emission cross sections for primary neutrons of (8.56 ± 0.19) MeV at 40° (a) and 120° (b) and of (12.72 ± 1.03) MeV at 120° (c). The dashed line is the 3-particle break-up contribution, the full line the sum of 3-particle break-up and 2-step reaction

often by as much as 15 % or more. The present data fluctuate more or less around the average of the evaluation. This is not true for the 24° scattering angle where above 7 MeV the present data are systematically lower by about 10 %, and for the 40° scattering angle where the results are systematically higher between 3 and 10 MeV. Above 12 MeV the data are lower for all angles except at 40°. As summarized in Fig. 21 it has been tried to parameterize the 'continuum' neutrons by distinguishing between:

- inelastic scattering (n,n_2), (n,n_3)
- 3-particle break up $(n,n'\alpha t)$
- 2-step reaction $(n,t)^5He \rightarrow \alpha+n'$.

The resulting angle-integrated (n,n_2) cross sections are higher than several recently published values (see Fig. 22). A paper for Nucl. Sci. Eng. is in preparation.

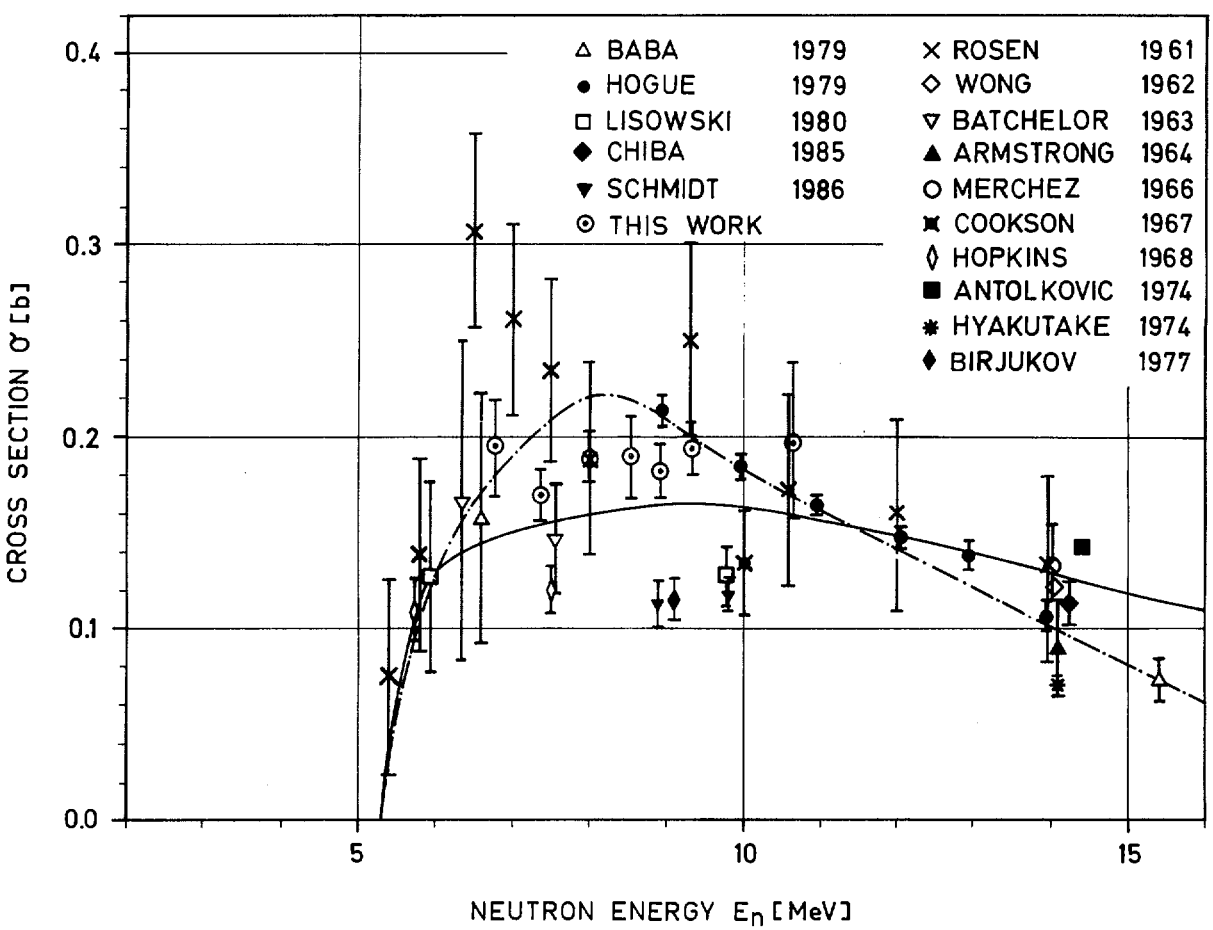

Fig. 22. Angle-integrated $^7Li(n,n_2)$-cross sections.
——ENDF/B-5; -·-·-·JENDL-3

Double Differential Neutron-Emission Cross sections for the ^{9}Be + n Reactions

E. Dekempeneer*, L. Mewissen**, F. Poortmans**, H. Weigmann

Beryllium is a candidate neutron multiplier for the blanket of a fusion reactor. Calculating the tritium breeding rate in the blanket requires a detailed knowledge of the energies and angular distributions of the neutrons emitted from beryllium through the elastic and various inelastic neutron channels.
A first series of measurements of double-differential neutron-emission cross sections have been started at GELINA, covering an incident energy range from 1.5 MeV up to 9 MeV.

Experimentally Determined Excitation Function for the ^{9}Be(n,t) Reaction

H. Liskien, R. Widera, S.M. Qaim*** and R. Wölfle***

The present work yields for the first time an experimentally determined excitation function for beryllium which - besides lead - is the candidate material for neutron multiplication in fusion reactors. Our present knowledge is based on 14 MeV values and theoretical calculations.
Two sets of eleven beryllium samples each have been irradiated with neutrons from the T(d,n)^{4}He-reaction. These neutrons were produced by bombarding a 3 mg/cm^2 T-Ti layer with a deuteron beam from the CN-type Van de Graaff accelerator at CBNM. The samples were sandwiched between two aluminium sheets 2 cm ø × 1 mm and suspended from a graduated ring which was adjusted with its centre above the source. The nominal distance between the source and the middle plane sample was 59.2 mm. The neutron fluence rate averaged over the sample volume and the irradiation time has been determined for each sample in two independent ways : 1) by using a proton-recoil telescope, and 2) by determining absolutely the ^{24}Na activity from the aluminium sheets which sandwiched the samples.
The irradiated samples were transported to KFA, Jülich where the induced tritium was quantitatively extracted and counted in a low-background gas proportional counter. The results disagree with the JEF-1 prediction but show a remarkably good agreement with the JENDL-3 and a recent evaluation made at LANL.

---

* Visiting Scientist from the Free University of Brussels, Brusssels, Belgium
** SCK/CEN, Mol, Belgium
*** KFA, Jülich, Germany

Sub-nanosecond Timing of α Particles with a Multi-Wire Parallel-Plate Avalanche Counter

E. Wattecamps and F. Arnotte

In view of (n, charged particle) cross-section measurements with the neutron source of 250 ps pulse width of the Van de Graaff accelerator, a low pressure multi-wire parallel-plate avalanche counter (MWPPAC) was designed and tested. The MWPPAC is made of a circular multi-wire anode plane of 5 cm diameter (gilded tungsten wires of 25 μm diameter every 0.8 mm) between two aluminised polycarbonate cathode foils of 150 $\mu g/cm^2$ thickness. The distance between anode and cathode is 3.5 mm. The counting gas is isobutane at 130 Pa, the voltage is 560 V and the estimated gas multiplication amounts to approximately $4 \cdot 10^4$. Two MWPPACs were mounted in line with a surface barrier detector, thus defining a telescope in front of an α-particle source of ^{241}Am. The fast detection chains of the MWPPACs are made of a preamplifier CANBERRA 2004, a fast amplifier SEN FTA-410L and a constant fraction timing discriminator ORTEC CFTD 934.

The rise time of the electron pulse on the anode is 8 to 12 ns and its height 10 to 30 mV, whereas the ion pulse has 1.5 μs rise time and about 100 mV at the output of the preamplifier. Proper adjustment of the damping of the charge integrator amplifier and pole zero adjust were essential to achieve the fast rise time. A time distribution of 5.5 MeV alpha particles passing the two MWPPACs gave a resolution of 690 ps at FWHM for a single detector chain. The optimum delay-line clipping for the CFTD was 150 cm cable RG 174U or 7 ns. The lower bias of the CFTD was varied between 0.2 and 1.0 V. Within this range the time resolution remains almost constant. The pulse-height resolution of a single MWPPAC amounts to 60 %. The sensitivity of the amplification to changes of the electric field was investigated in the vicinity of the stable working conditions. Relative amplitude changes, $\Delta V/V$, of 39 % per relative change of voltage, $\Delta U/U$, of 3%, were observed.

The stability in time was investigated by observing the time- and pulse-height resolution over 10 h. Whereas the pressure rises from 130 to 300 Pa, the time resolution gets broader from 690 ps to 1000 ps, and the pulse height decreases by 25 %. Developments are being made to improve the long term stability of a continuous gas flow system with pressure stabilisation.

Measurements of Double-Differential (n,α) Cross Sections

E. Wattecamps, F. Arnotte
(WRENDA request N°s 801147, 78106, 781064)

Measurements of double-differential (n,α) cross sections of nickel and copper were made at the Van de Graaff in the neutron energy range from 5 to 10 MeV in steps of 0.5 MeV. Some results were presented at the International Conference on Fast Neutron Physics, Dubrovnik, May 1986. The alpha-particle yield data are compared to data available in the literature and in particular to the recommended sets ENDF/B-5, JEF-1 and JENDL-2. This comparison points to the agreement between experimental data obtained by various techniques but also indicates significant differences from the ENDF/B-5 data. In particular the results from (n,α) measurements of elemental nickel are quite different from evaluated data ; whereas the Cu(n,α) data agree rather well with evaluated data. To resolve this discrepancy measurements of (n,α) reaction-rate ratios of single isotopes were started : ^{60}Ni to ^{58}Ni and ^{63}Cu to ^{58}Ni were measured and plans are made to measure ^{65}Cu to ^{58}Ni and ^{58}Ni to nickel also. Measured (n,α) cross section ratios of ^{60}Ni to ^{58}Ni are shown in Fig. 23 together with the ratios deduced from the evaluations JENDL-1, JENDL-2; and togetherwith experimental data obtained elsewhere[1-3].

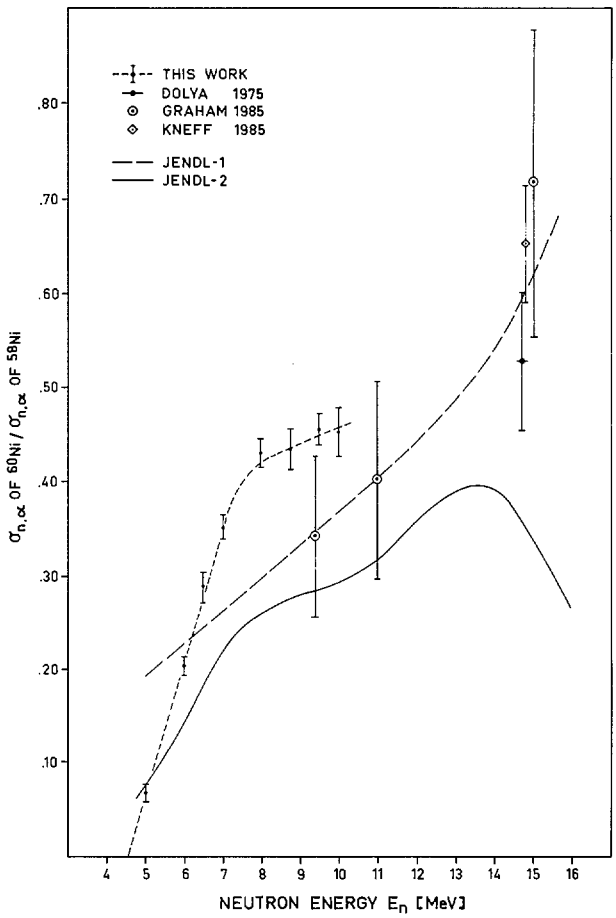

Fig. 23. Comparison of measured (n,α) cross-section ratios of ^{60}Ni to ^{58}Ni as a function of neutron energy with the evaluations and earlier measurements

Our ratios are quite larger than the ratios deduced from the JENDL evaluations, and are larger, but still

(1) G.P. Dolya, A.P. Klyucharer, V.P. Bozhko, V.Ya. Golovnya, A.S. Kachan and A.I. Tutubalin, 3rd AU-Union Conf. Neutron Physics, Kiev, Pt. 4 (1975) p. 173
(2) S.L. Graham, M. Ahmad, S.M. Grimes, H. Satyanarayana, and S.K. Saraf, Nucl. Sci. Eng. 95 (1987) 60
(3) D.W. Kneff and L.R. Greenwood, INDC (NDS)-179/G (1986) p. 61

consistent, within the error margins, with the data of Graham et al.[1]. Measurements at 14 MeV and the analysis of the reaction-rate ratio measurements of ^{63}Cu to ^{58}Ni are in progress.

---

(1) S.L. Graham, M. Ahmad, S.M. Grimes, H. Satyanarayana, and S.K. Saraf, Nucl. Sci. Eng. 95 (1987) 60

1.4 SPECIAL STUDIES

Nuclear Quadrupole Interaction of Fluorine in Intercalated Carbon Compounds

C. Budtz-Jørgensen, P.W. Martin*, G. Hooley*

The final evaluation of the measured hyperfine quadrupole-interaction data reported previously[1] has been started at the University of British Columbia, Vancouver and a paper on the subject is in preparation.

Neutron-Resonance Spectroscopy of ^{28}Si + n

P.W. Martin**, L. Mewissen***, F. Poortmans, J.A. Wartena, H. Weigmann

In the frame of a systematic study of the basic properties of neutron-resonance reactions, the total and partial radiative capture cross sections of ^{28}Si have been measured. This nucleus is known as a test case for intermediate structure phenomena, and it also may be expected to show a relatively large magnetic-dipole strength which recently has received much theoretical interest.

Experimental details have been described in the preceding progress report.[2] A detailed resonance-parameter analysis has been carried out up to a neutron energy of 2.75 MeV. Level densities have been determined for s- and p- wave resonances, as well as neutron-strength functions and partial radiative widths. The neutron strengths have been compared with existing model calculations, and doorway-type structures have been observed in several neutron channels.

The neutron width of at least one T = 3/2 level has been determined, providing a measure of isobaric spin mixing. Whereas other workers previously reported a strong correlation between the reduced neutron widths (Γ_n^l) and total radiative widths, we observe no significant correlation between Γ_n^l and the partial radiative widths for ground state transitions. We conclude that radiative capture in ^{28}Si +n does not proceed via a simple valence mechanism, but must involve several competing

---

* University of British Columbia, Vancouver, Canada
** Visiting Scientist from the University of British Columbia, Vancouver, Canada
*** SCK/CEN, Mol, Belgium

(1) NEANDC (E) 272 "U" Vol. III Euratom; INDC (EUR) 020/G (1986), p. 53
(2) Ibidem, p. 50

doorway states. The observed M1 strength in ^{29}Si is lower than that reported for ^{28}Si from inelastic electron scattering, suggesting either a considerable fragmentation or a significant reduction due to the presence of the additional neutron.

The $^{33}S(n,\alpha)^{30}Si$ Reaction in the Resonance Region

C. Wagemans*, H. Weigmann, R. Barthélémy

As a part of a systematic investigation of the (n,p) and (n,α) reactions in the resonance region, the $^{33}S(n,\alpha)^{30}Si$ reaction has been studied. This reaction is of particular interest for astrophysics since it has a direct impact on calculations of explosive nucleosynthesis. Starting from the conversion of ^{32}S and ^{36}Ar initially present in a star during explosive carbon burning, calculations lead to an overproduction of the neutron-rich isotope ^{36}S. Since $^{33}S(n,\alpha)$ is the main destructive reaction in the reaction sequence considered in these calculations, reliable $^{33}S(n,\alpha)$ cross section data are required.
The measurements have been performed up to 1 MeV neutron energy, and a resonance-parameter analysis yields α-widths Γ_α or values of $g\ \Gamma_n\ \Gamma_\alpha/\Gamma$ for 16 resolved resonances up to 400 keV. The resonance spins are known for most of the observed resonances due to combined information from transmission[1] and the present (n,α) measurements.
The Maxwellian averaged (n,α) cross section is smaller than that deduced from earlier data. Thus, it fails to explain the discrepancy between the measured and calculated stellar abundance of ^{36}S.

Neutron Resonance Spectroscopy of $^{207}Pb + n$

R. Köhler**, L. Mewissen*, F. Poortmans*, S. Raman***, J.A. Wartena, H. Weigmann

Lead is a possible candidate to be used as a neutron multiplier in fusion reactor blankets. Therefore the cross sections of lead isotopes have to be known, and for evaluations on the basis of nuclear-model calculations the basic statistical properties of ^{208}Pb (nuclear-level densities, neutron

* SCK/CEN, Mol, Belgium
** EC Fellow
*** ORNL, Oak Ridge, Tenn., USA
(1) G. Coddens, M. Salah, J.A. Harvey and N.W. Hill, to be published.

and radiative strength functions) are required. The present measurements were also undertaken in order to search for the physically interesting magnetic-dipole strength. Experimental details can be found in the preceding progress report [1].

A detailed resonance-parameter analysis has been carried out up to a neutron energy of 700 keV. The nuclear-level density shows a strong parity dependence. The doorway in the s-wave neutron-strength function has been firmly established with an escape width equal to the corresponding widths in the neighbouring isotopes. The total magnetic-dipole strength detected between the neutron-separation energy and 8.0 MeV is $B(M1)\uparrow = 5.8\ \mu_0^2$, thus smaller than the lowest theoretical estimate for that region. Above that energy an additional $1\ \mu_0^2$ is observed, but more strength may have escaped detection because the sensitivity of the experiment decreases; hence, the "missing" strength may be partly hidden at these higher energies. Radiative widths for the E1 decay of resonances to the first-excited state of ^{208}Pb show a doorway structure which can be related to the properties of known bound states.

The Properties of Intruder States Studied with Cd-Isotopes

G. Rohr

A talk with this title has been presented at the "50. Physiker Tagung" in Heidelberg 1986. The main content of the talk is collected in Fig. 24 which contains two sorts of data:

1) a systematics of the first excited levels of cadmium. The 0^+ states which are connected with dotted lines are considered as intruder states. They approach the energy of the two-phonon triplet for the cadmium isotopes 112 and 114, and
2) the pairing energies of the excited nuclei Δ_{EXI} are presented by shorter bold lines and are connected with solid lines. They are derived from the level density of neutron resonances: the corresponding level density parameter "a" calculated from the Bethe level-density formula, deviates from the base line[2] (Fig. 25). This deviation is a measure of a change of the pairing energy at high excitation compared to the ground state value as measured by mass differences.

---

(1) NEANDC (E) 272 "U" Vol. III Euratom; INDC (EUR) 020/G (1986), p. 51
(2) G. Rohr, Z. Phys. A 318 (1984) 299

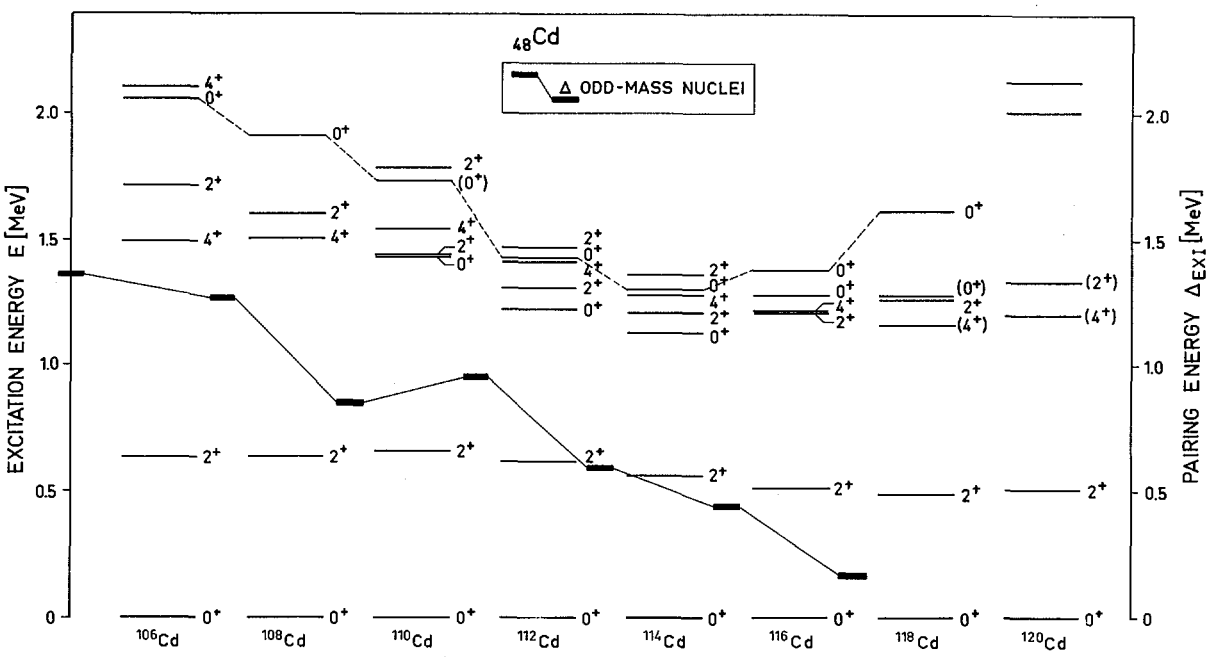

Fig. 24. Systematics of low excited states for Cd isotopes and the pairing energy determined at neutron separation energy

The reduction in the pairing energy is caused by proton-neutron interaction and according to the independent-particle model results in a shift of all intrinsic states. The similarity of the energy behaviour of the 0^+ states (dotted lines) and of the pairing energy at high excitation (solid lines) as a function of the neutron number indicates that the intruder states are of single-particle character. There is no need for the introduction of a new type of excitation[1].

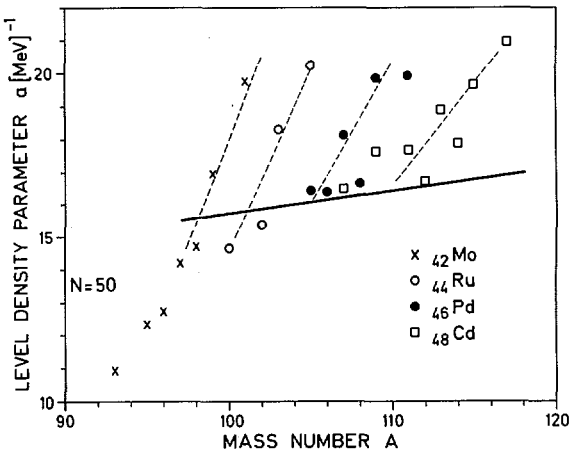

Fig. 25. The level density parameter for nuclei with A ≈ 108; base line: solid curve

(1) K. Heyde, P. Van Isacker, R.F. Casten and J.L. Wood, Phys. Lett. 155B (1985) 303

The higher energy of the intruder states in ^{118}Cd and ^{120}Cd can be explained by a shell effect. According to the Nilsson model the sequence of the single-particle states between the neutron shells 50 and 82 are $g^{7/2}$, $d^{5/2}$, $s^{1/2}$, $d^{3/2}$ and $h^{11/2}$. The mutual polarization mechanism[1] will change the sequence of occupation in a way that $s^{1/2}$ and $h^{11/2}$ are filled last. Thus, for a nucleus with N > 70 all neutron states with the same parity as the proton states are filled and the p-n interaction has disappeared. Therefore the intruder states are not perturbed and they are expected at higher energy.
The energy of the unperturbed state in ^{120}Cd at 2.034 MeV is a 0^+ state; its energy varies with the energy of the intruder state in ^{106}Cd. The smaller perturbation of the intruder state in ^{118}Cd can be explained with a reduction of the p-n interaction compared to ^{106}Cd. The last neutrons occupy the $s^{1/2}$ states and the spin-orbit partner orbitals of $1g^{9/2}(\pi)$ and $3s^{1/2}(\nu)$ have a large difference in angular momentum, resulting in a smaller p-n interaction.
The cadmium spectra provide the best example of intruder states in this mass region. For the isotopes of molybdenum, ruthenium and palladium more measurements at higher excitation energy are needed.

Observation of Level-Density Discontinuities for ^{50}Cr, ^{52}Cr

G. Rohr, R. Shelley, A. Brusegan, F. Corvi, L. Mewissen*, F. Poortmans*

The resonance data presented at the Santa Fe Conference (1985) and the results of an extension of the analysis of transmission data for ^{52}Cr up to 1 MeV, made a new interpretation of resonances possible. In total 295 and 202 resonances, of which 60 and 24 are of s-wave character, have been analysed for ^{50}Cr and ^{52}Cr, respectively. From the experience with the procedure MISDO, which determines the number of missed s-wave resonances, it could be concluded for the high resolution measurements, that all s-wave resonances are detected.
^{50}Cr: The s-wave level density D_0 calculated for bins of 200 keV is included in Table 2., wherein N is the number of resonances and a is the level-density parameter.

---

* SCK/CEN, Mol, Belgium
(1) P. Federman and S. Pittel, Phys. Rev. C20 (1979) 820

Table 2. Excited levels in ^{50}Cr

Energy range[keV]	N	D_0 [keV]	a [1/MeV]
0 - 200	11	18.2 ± 2.9	6.21 ± 0.12
200 - 400	11	18.2 ± 2.9	6.15 ± 0.12
400 - 600	16	12.5 ± 1.6	6.47 ± 0.18
600 - 800	22	9.1 ± 1.0	6.72 ± 0.25

The change in the level spacing in the (600-800) keV interval by a factor of two compared to that of (0-200) keV can be interpreted by the level-density systematics[1]. The corresponding level-density parameter changes from a = 6.2 to 6.7. The values are between the level-density parameter for doorway states a_{2p1h} = 5.3 and a_{3p2h} = 7.4 Therefore the experimental level-density parameter is in the transition region where the energy is high enough for the excitation of 3p2h states. In this case an additional energy dependence, much stronger than that of the Bethe level-density will arise. The occurence of this effect at the compound nucleus A = 51 (N = 27) is due to the neutron shell closure.

^{52}Cr: The results of the analysis of the transmission data can be compared with recent ORNL data[2] up to 910 keV. There, 20 resonances are assigned as s-waves, three of which are interpreted at CBNM as p-wave resonances, namely at 251, 653 and 766 keV. However, some additional four resonances can be assigned as s-waves, giving a total of 21 resonances. The average level spacing D_0 = (41.5 ± 3.0) keV is in agreement with the ORNL results. As shown in Fig. 26 the s-wave level distribution is not as linear as might be expected. Two gaps are apparent, at (140-265) keV and (612-740) keV, where at least two resonances for each gap are

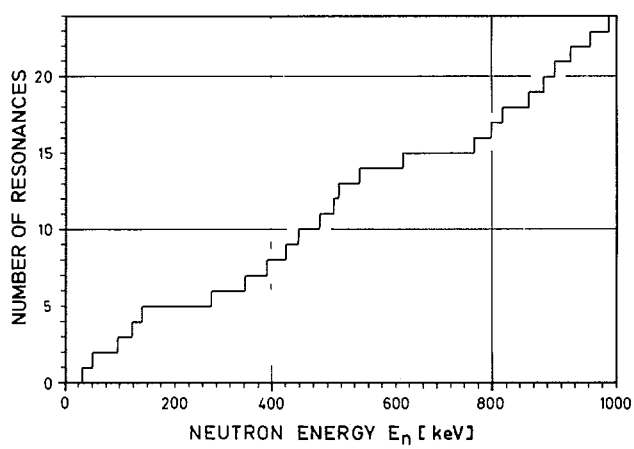

Fig. 26. Number of ^{52}Cr s-wave resonances as a function of neutron energy

(1) G. Rohr, Z. Phys. A318 (1984) 299

(2) H M. Agrawal, J.B. Garg and J.A. Harvey, Phys. Rev. C Vol. 30 (1984) 1880

missing. The first gap is also observed at ORNL. The probability of having two such gaps has been estimated to be 0.2%, by means of a Monte Carlo code based on a Wigner distribution. The probability of having a single gap is 2%. Another even stronger discontinuity of the level spacing is observed for p-wave resonances as shown in Fig. 27. If the resonances up to 500 keV are considered and only p-wave resonances are assigned, two regions can be distinguished where the level spacing distribution is linear, namely the intervals (0-200) and (300-500) keV. The ranges are separated by a clustering of p-wave resonances at 250 keV. The strong increase of

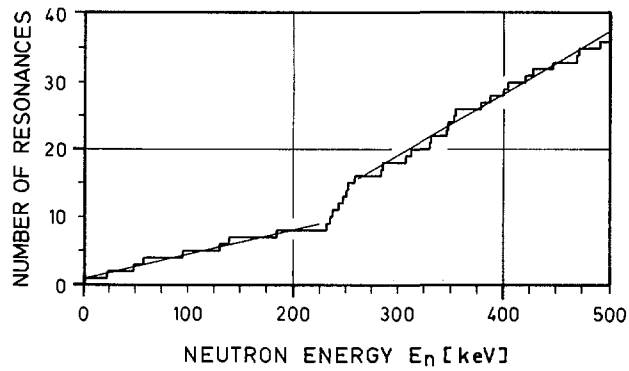

Fig. 27. Number of ^{52}Cr p-wave resonances as a function of neutron energy

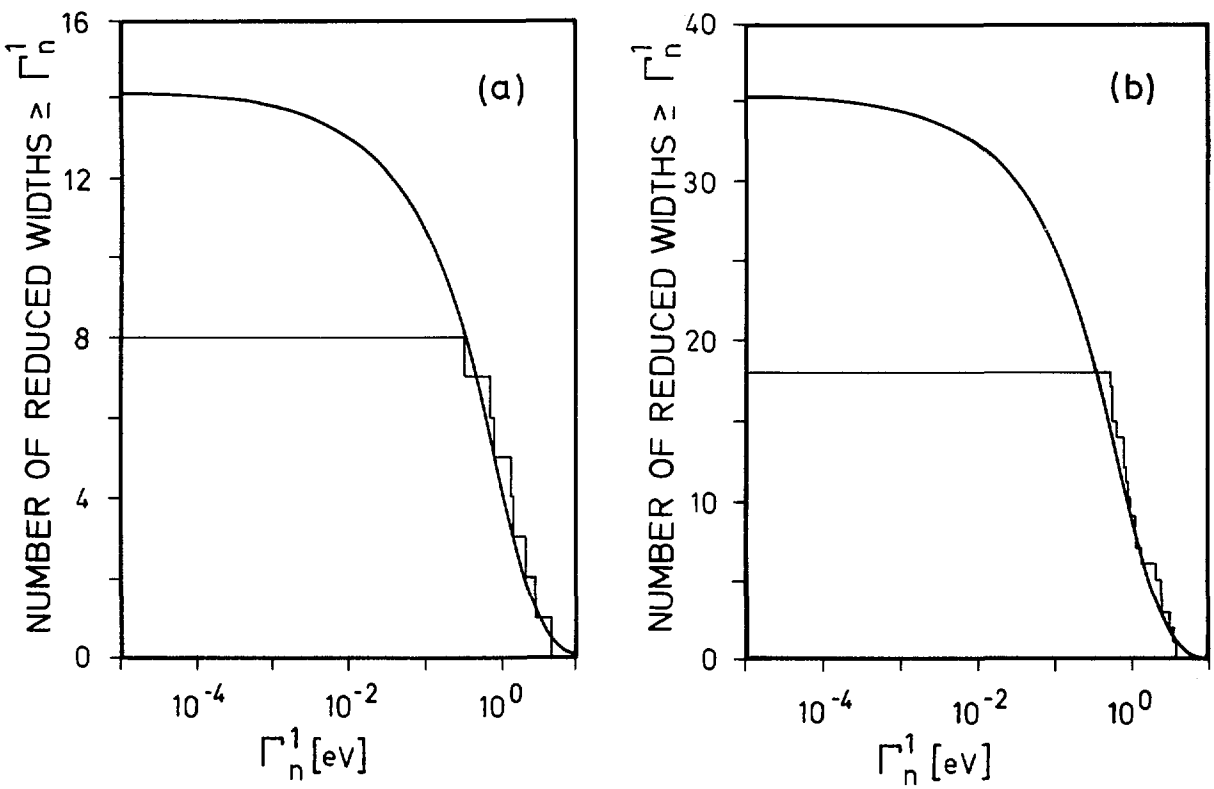

Fig. 28. Histograms of reduced neutron widths for ^{52}Cr p-wave resonances fitted with Porter-Thomas distributions; (a) energy range: (0 - 200) keV, (N = 14 ± 4); (b) energy range:(300 - 500) keV, (N = 35 ± 5)

levels at about 250 keV can be interpreted as a threshold for additional resonances with higher hierarchy as discussed above for ^{50}Cr resonances.
The level spacings in the intervals (0-200) and (300-500) keV have been estimated by individual fitting with a Porter Thomas distribution (Fig. 28a and b) for the reduced widths.
The results were D_1 = 14.7 keV and D_1 = 5.7 keV respectively. However, as expected there is no change of the p-wave strength function except for the accumulation of resonances at 250 keV. The p-wave level spacing D_1 = 14.7 keV for the lower interval (0-200) keV is by a factor 3 smaller than the observed s-wave spacing and in agreement with the level statistics. However, in the interval (300-500) keV there are 2.6 times more p-wave than s-wave resonances indicating a local parity dependence. In the ORNL publication a parity dependence for the whole measured range has been stated.

2 NUCLEAR METROLOGY

2.1 RADIONUCLIDE METROLOGY

Low-Energy X-Ray Standards

B. Denecke, G. Grosse, W. Oldenhof

Two excitation sources were prepared by covering ^{55}Fe (185 MBq) sources with Al foils. These sources were measured with a proportional counter in a defined solid angle. There were, however, difficulties concerning the stability and reliability of the results due to electromagnetic interferences (EMI) on the electronics and problems with gas permeability of the counter window. The signal-to-noise ratio could be improved considerably by a special non-overloading charge-sensitive preamplifier. The EMI problems could be reduced by a carefully designed shielding and the application of transient-suppressing isolation transformers. A new type of counter window consisting of laminated plastic and carbon films was fabricated.

4π-CsI(Tl)-Sandwich Spectrometer

B. Denecke

The 4π-CsI(Tl)-sandwich-detector system, consisting of two independent scintillation crystals for measurements of photons between 10 and 200 keV is applied to the study of the 60 keV γ-ray emission probability in the decay of ^{241}Am and was utilized successfully in two international comparisons to measure the activity concentration of ^{109}Cd solutions.
Due to the absence of absorbing windows in front of the detectors electron emission rates could be measured with nearly 100% efficiency with an accuracy of about 0.4%.
Effort was made to improve the prototype spectrometer, in particular the access to the source position, the operation readiness of the spectrometer, the stability of the measurement and the reliability of the results.
A light-tight interlock was constructed to keep the spectrometer continuously in complete darkness, at dry conditions and under high voltage supply. Both detectors can be moved separately with respect to the source by various distance flanges. Light- and gas-tight shutters confine the detectors in their housings in a hydrogen flow. This allows to change the

sources and absorbers conveniently maintaining safe and stable operation of the spectrometer.
In addition, the signal processing of the associated electronic system has been improved. High-energy background pulses are followed by a cascade of many small pulses during some milliseconds which superimpose on the Poisson-distributed pulses originating from the radionuclide decay. This effect disturbs the proper life-time measurement and causes errors on the measured countrates. Its influence was eliminated by an extension of the deadtimes of both the ADC and the scaler chain by several milliseconds for every detected pulse exceeding 500 keV. By this measure consistent results of the countrates in the spectrum and scalers were obtained.

Ionization Chamber

D. Reher, C. Ballaux*, E. Celen

Calibrated ionization chambers are widely used in nuclear medicine to determine the radioactivity of γ-ray-emitting radiopharmaceuticals. In radionuclide metrology pressurized ionization chambers are used for various purposes: to retain the calibrations for γ-ray emitters, to check the consistency between results of different measurements made at different times, to test dilution and sampling methods, and to accumulate half-life data. These chambers provide an efficient tool for a calibration service and for the definition of radioactivity reference materials.
Ionization chambers are only useful instruments as long as their calibration figures remain stable for a long period of time. At CBNM an ionization chamber (20th Century, type IG-12) filled with 2 MPa of argon was installed and several properties of the system were tested.
Usually the average ionization current I produced in the chamber is measured by the change of the voltage ΔU during time interval Δt using an electrometer amplifier and an integrating capacitor

$$I = C\frac{\Delta U}{\Delta t}$$

The proportionality factor C, the capacitance, is of fundamental importance for the stability.
Air capacitors, similar to the design of Giebe[1] were constructed at CBNM's

* SCK/CEN, Mol, Belgium
(1) E. Giebe, Z. Instrum. 29, (1909) 269 and E. Giebe, G. Zickner, Z. Instrum. 53 (1933) 1, 49, 97

workshop. Fig. 29 shows a schematic view of the capacitor of the type also used at the NPL, Teddington. This type of capacitor is very stable. The capacity changes were found to be less than 0.1 % within three months.

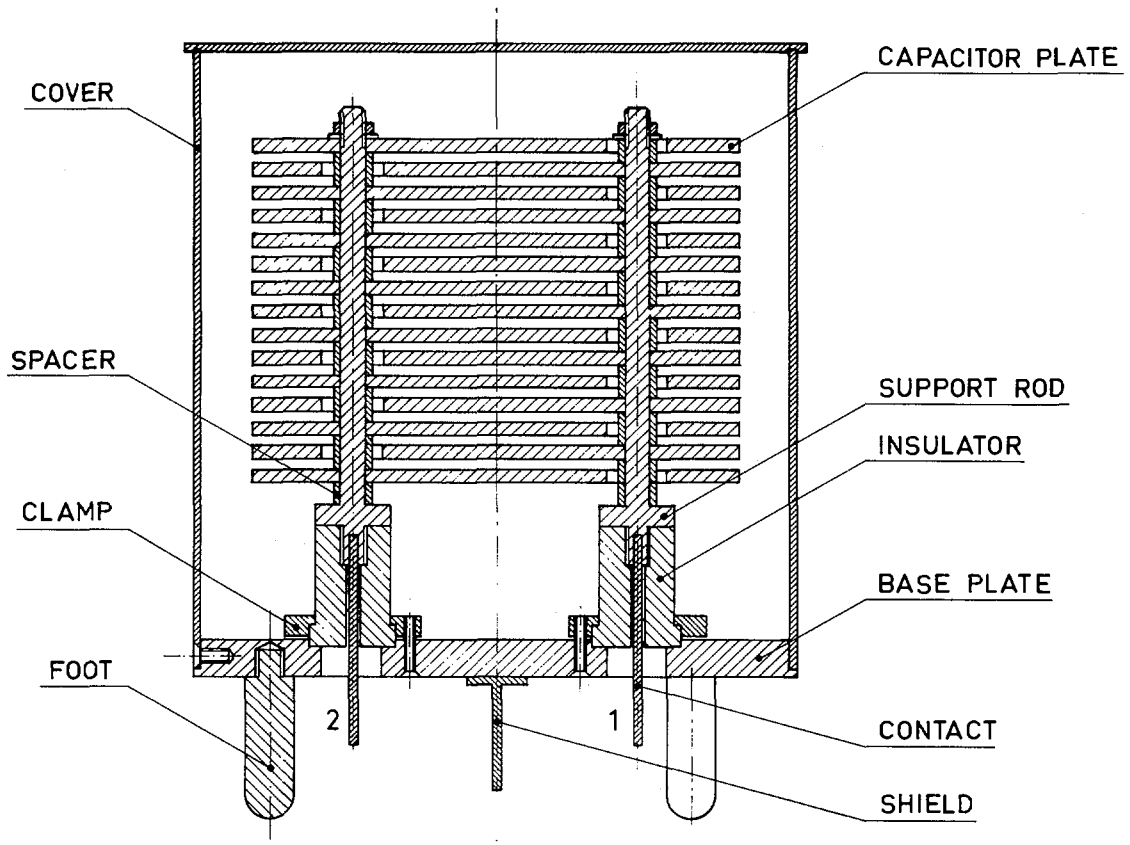

Fig.29. Schematic view (vertical cut) of the 500 pF air capacitor used at CBNM

The axial and the radial response of the chamber were measured using ^{226}Ra standard sources and various liner materials. The smallest variation of the efficiency was found with a lucite adapter. This is important for measurements of solutions in ampoules of different filling heights. Fig. 30. shows the results of these measurements.

Background current ($i_{backg.}$ = 46 fA) does compare well with those measured at other standards laboratories. It is a measure of the sensitivity of the current-measuring system.

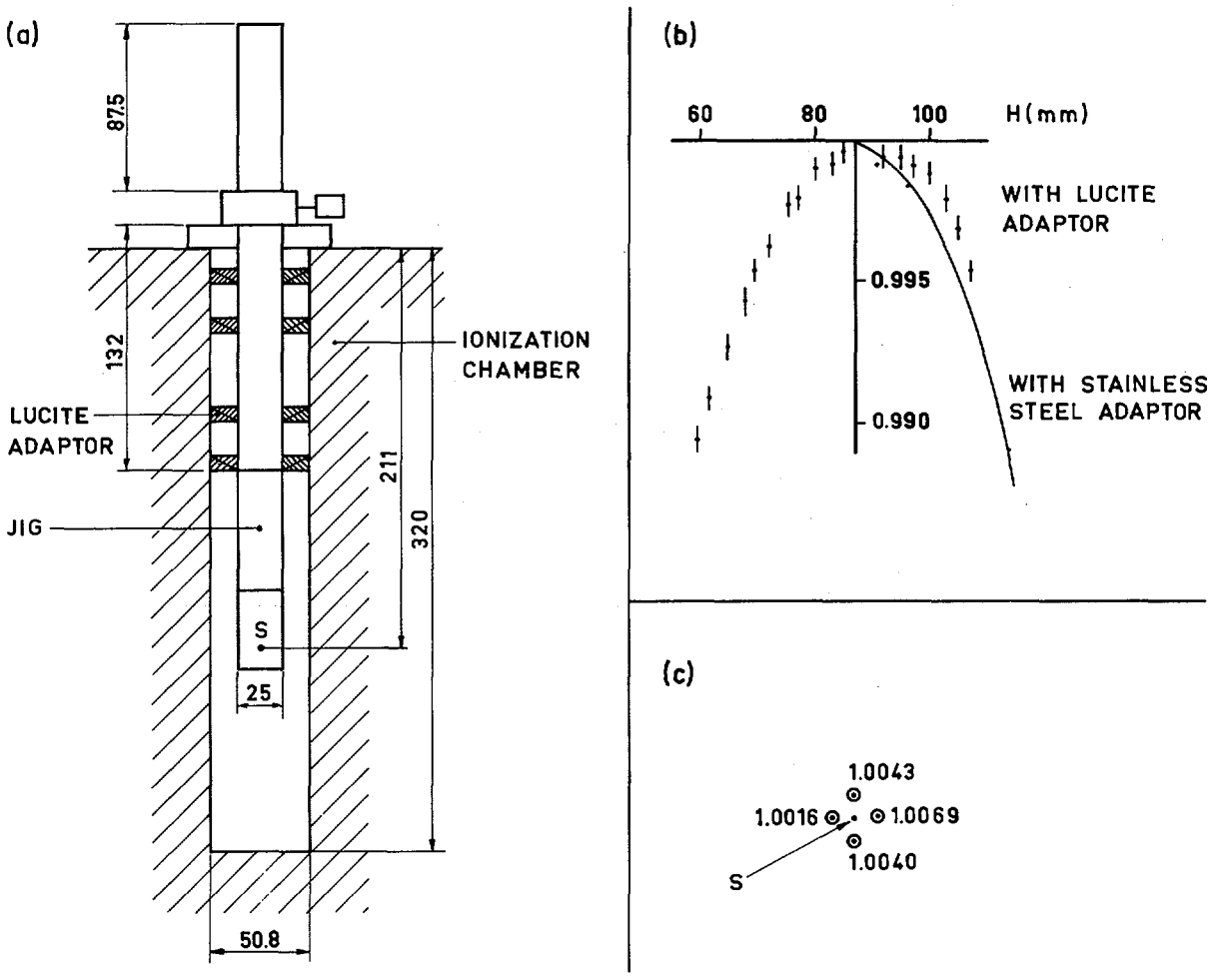

Fig. 30. Sectional view of the ionization chamber and relative variations of the ionization current as a function of the displacements of the reference source in axial and radial directions:

(a) Well for the ionization chamber, covered with the lucite adaptor (132 mm length) and with the lucite jig. S is the position of the reference source;

(b) Axial response fo the ionization chamber: for H = 87.5 mm, the source is located 211 mm below the top of the chamber;

(c) Radial response of the ionization chamber: the relative currents are given in the four directions, when the source is moved 4 mm from the point S. In S, the current is 1.000

International Comparison of Activity-Concentration Measurements of a ^{109}Cd Solution

D. Reher, B. Denecke, C. Lievens, W. Oldenhof

As a follow-up of the trial intercomparison of activity concentration measurements of a ^{109}Cd solution, which was performed in 1985, CBNM participated in a large-scale intercomparison on the same radionuclide. The comparison was organized on behalf of Section II (Mesures des Radionucléides) of the CCEMRI by the BIPM, Paris. Besides CBNM, 22 labora-

tories participated in this intercomparison. The ^{109}Cd solution was distributed by the OMH, Budapest, and checked for impurities by the NAC, Faure, and the IER de l'EPFL, Lausanne.
Each participant received one flame-sealed NBS-type ampoule containing about 3.6 g of solution with a ^{109}Cd activity concentration of about 5.6 $MBq \cdot g^{-1}$ in an aqueous solution of HCl (0.1 $mol \cdot dm^{-3}$).
At CBNM two different methods were employed for the standardization: 1) a 4π-CsI(Tl)-sandwich spectrometer was used to measure the disintegration rate of four ^{109}Cd sources which were prepared from two dilutions of the original solution, and 2) a 4π proportional counter operated at high pressure was used. Eight sources were measured at 0.3, 0.4, and 0.5 MPa of Ar-CH_4 (9:1) as counting gas. The results obtained at CBNM are listed in Table 3.

Table 3. Results of the ^{109}Cd measurements

Method	Standard deviation [%]	Activity concentration on March 1st, 1986 [$MBq \cdot g^{-1}$]
4π CsI(Tl)	0.1	5.980 ± 0.024
4π Proportional counter	0.2	5.967 ± 0.020

There is an excellent agreement of CBNM results with those of the other laboratories as shown in Fig. 31.

Development of a Tracer Technique for the Standardization of ^{109}Cd

D. Reher, E. Celen, C. Ballaux*

Coincidence counting of mixed sources ^{109}Cd-^{65}Zn and ^{109}Cd-^{203}Hg was performed with CH_4 and Ar-CH_4 (9:1) as counting gases for the flow-proportional counter. With ^{65}Zn and ^{203}Hg as tracers, efficiencies ε_β were achieved up to 0.31 and 0.92, respectively. The scatter of the extrapolated values $N_{\beta o}$ was always much larger than the statistical uncertainties. This indicates that the sources were probably not sufficiently homogeneous. Furthermore, quite

* SCK/CEN, Mol, Belgium

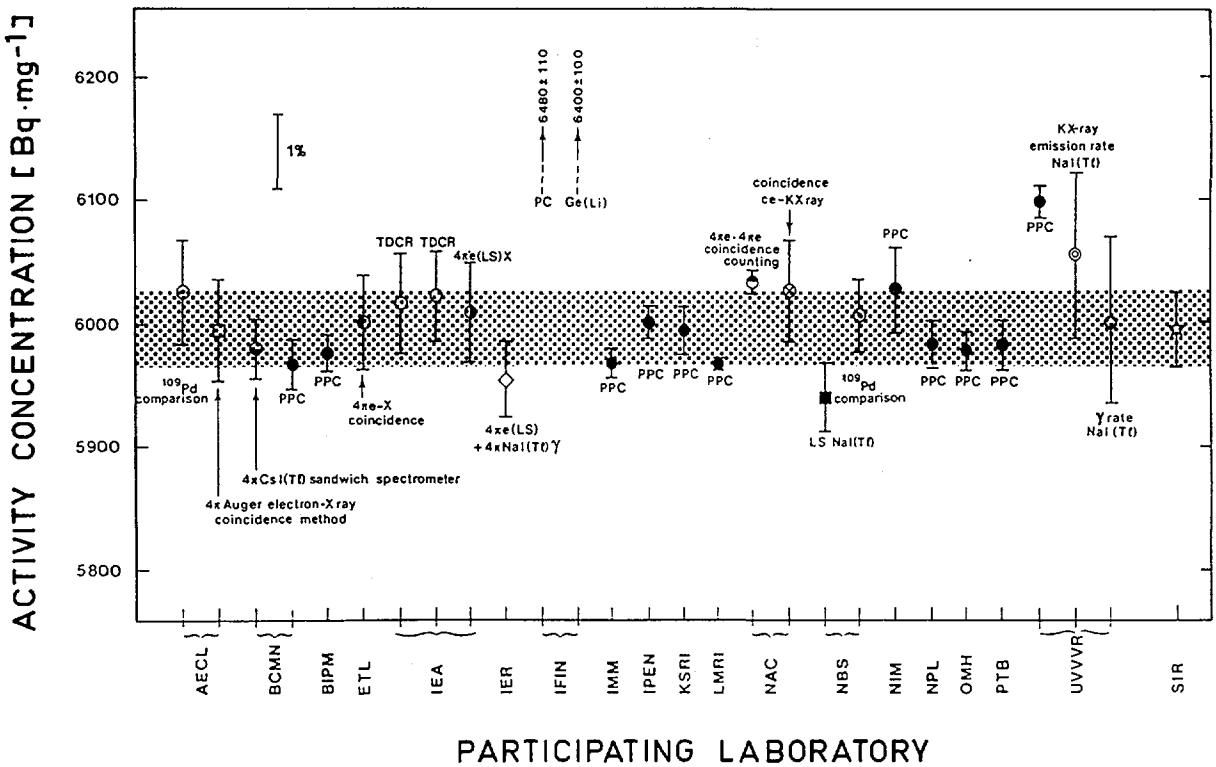

Fig. 31. Graphical representation of the results of the ^{109}Cd intercomparison

large differences of about 10% were observed for the slope of the efficiency function and for the source self absorption. At least in certain experimental conditions the efficiency function did not remain linear.

With ^{203}Hg as tracer and CH_4 as counting gas $N_{\beta o}$ was independent of the discriminator setting. Two factors posed problems: 1) the proportionality constant K between $N_{\beta o}$ and the activity of ^{109}Cd cannot simply be computed from the counting equations, due to pronounced coincidence-summing effects. These effects arise from the events of a cascade of vacancies, occuring in higher shells, after K- and L-electron capture by the nucleus and 2) the efficiency function for pure ^{203}Hg remains no longer linear when discriminating above 2.0 keV.

With ^{203}Hg as tracer and Ar-CH_4 as counting gas the discriminator was set at 11.8 keV. This is just between the energies of the KX rays and the K-Auger electrons originating from electron capture (EC) and those of the electrons originating from the internal-conversion process (IC). The efficiency function was measured above ε_β = 0.5. In this case K is simply $\alpha/(1+\alpha)$, where α is the total internal-conversion coefficient. The poor reproducibility was attributed to the limited separation of the two types of events (EC and IC). Therefore better results are expected with a pressurized proportional counter. Such a coincidence counting system is under construction.

2.2 METROLOGY OF NEUTRON FLUX AND DOSE

Neutron Calorimetry

A. Paulsen, H. Nerb, R. Widera

As a first step into neutron absorbed-dose calorimetry a graphite absorbed-dose calorimeter was constructed to be used in γ-ray and electron beams. This type of calorimeter was chosen because there is some relevant experience available in Europe. Thus, the performance of this calorimeter will be compared with those in the other laboratories and it will be applied at CBNM to calibrate the γ-ray beam of a 250 Ci ^{137}Cs source. This source will be used for ionization-chamber calibrations in order to determine the dose sharing in mixed neutron/γ-ray fields.

In 1986 the CBNM graphite calorimeter was put into operation and characteristic parameters, e.g. heat-transfer coefficients, heat loss corrections, calibration factors were experimentally determined. In Table 4 the calibration factors and heat-loss corrections are summarized for measuring periods of 100, 200, 400 and 800 s and for three different modes of operation: heat-loss compensated and quasi-adiabatic (electrical heating of core and jacket) with one and two heat sensors in the core. The results are satisfying, especially if one takes into consideration that the calorimeter will be mainly used in quasi-isothermal measurements in which electrical heating for calibration and irradiation is alternatively applied. A small dependence of the calibration factor on the length of the measuring period is observed and up to now unexplained. Furthermore, the experimental heat-loss corrections are larger than those calculated from the measured heat-transfer coefficients. Also this fact is unexplained up to now.

The construction of the tissue-equivalent plastic (TEP) calorimeter for application in neutron dosimetry was finished and the instrument was put into operation. In comparison with the graphite calorimeter it has the same number of calorimeter bodies (core, jacket, shield and medium), however, in the TEP calorimeter the shield is thermo-regulated and the medium forms a freely drifting buffer. Consequently, from the point of view of theoretical treatment, the TEP calorimeter forms a two-body calorimeter. All relevant computer codes have been accordingly modified.

Difficulties with the thermo-regulation of the shield have finally been solved by electronic adaptations in the thermostat amplifier. The shield

Table 4. Experimental calibration factors and heat-loss corrections for the CBNM graphite calorimeter

Mode of operation	Experimental quantity	Length of measuring period [s] 100	200	400	800	Mean calibration factors [Gy/V]
Heat loss compensated	Calibration factor [Gy/V]	8.7892	8.7979	8.7762	8.8264	8.7974
	SEOM* [Gy/V]	0.0021	0.0061	0.0010	0.0012	0.0106
(C1 + J)	Heat-loss correction [%]	0.406	0.974	3.586	9.334	--
	SEOM* [%]	0.014	0.009	0.002	0.023	--
Quasi-adiabatic	Calibration factor [Gy/V]	8.7960	8.8159	8.7675	8.8180	8.7993
	SEOM* [Gy/V]	0.0052	0.0001	0.0059	0.0011	0.0117
(C1)	Heat-loss correction [%]	0.377	0.895	3.497	9.290	--
	SEOM* [%]	0.023	0.025	0.122	0.023	--
Quasi-adiabatic	Calibration factor [Gy/V]	4.3859	4.3986	4.3689	4.4095	4.3907
	SEOM* [Gy/V]	0.0015	0.0014	0.0100	0.0007	0.0087
(C1 + C2)	Heat-loss correction [%]	0.337	0.923	3.293	9.623	--
	SEOM* [%]	0.030	0.047	0.422	0.148	--

*SEOM = Standard Error of the Mean

temperature of about 27.2°C stays constant within $2 \cdot 10^{-3}$ °C for 24 h. Additional measurements of the heat-transfer coefficients, the heat-loss corrections and the calibration factors are still going on.

International Fluence Comparison

H. Liskien, A. Paulsen, R. Widera, S. Bao*

Neutron fluence-rate determination is a key issue in neutron metrology. International fluence comparisons between standardizing laboratories (or the equivalent) of many countries are organized under the auspices of CCEMRI/BIPM. Table 5 summarizes information about the presently ongoing comparisons.

Table 5. Summary of ongoing neutron fluence comparisons

Transfer method	Coordi-nation	Neutron energy [MeV]				
		0.144	0.565	2.5	5.0	14.8
^{115}In(n,n') activation	CBNM	0	0	+	+	+
^{93}Nb(n,n') activation	NPL	0	0	0	0	+
^{115}In(n,γ) activation	NPL	-	+	0	0	0
^{235}U(n,f) FF* counting	AERE	-	+	+	+	+
^{238}U(n,f) FF* counting	AERE	0	0	+	+	+

0 not applicable
+ applicable, CBNM participated
- applicable, CBNM did not participate
FF* = fission fragment

The results of the first two campaigns have been published in 1984. The results of the third exercise were evaluated by the NPL, Teddington in 1986 and are briefly discussed below. A manuscript has been accepted by Metrologia. The last two comparisons are presently executed and CBNM hascarried out its measurements during January/February 1986. These measurements are also briefly described below.

An international comparison of neutron fluence rate at 144 and 565 keV was organized by the NPL, Teddington. Small indium foils were used as the trans-

---

* Visiting Scientist from University Beijing, Beijing, PR of China

fer medium, the induced radioactivity from the $^{115}In(n,\gamma)^{116m}In$ reaction being assayed with a $4\pi\beta$ counter. For intensity reasons CBNM participated only at 565 keV neutron energy. The quantity to be compared is the specific activation countrate at the end of irradiation $A_1[s^{-1}\cdot g^{-1}]$ divided by the product of the neutron flux density ϕ $[s^{-1}\cdot cm^{-2}]$ and the saturation factor S:

$$R = \frac{A_1}{\phi \cdot S} \left[cm^2 \cdot g^{-1} \right]$$

The final results at 565 keV neutron energy are plotted in Fig. 32 for the six laboratories having participated.

The data shown in Fig. 32 have a spread of 7.6 % which is unexpectedly high. A least squares analysis indicates a distorted distribution. As a result of this intercomparison, it has also been found that neutron scattering in the target backing, when using the $^7Li(p,n)$ reaction as a source of neutrons in the energy range 100 to 600 keV, has apparently been underestimated in the past. This can have a large effect on activation-capture cross-section measurements.

At the beginning of 1986 CBNM carried out at the 7 MV Van de Graaff accelerator the measurements required for the two last intercomparisons as indicated in Table 5. In these intercomparisons multiplate-ionization chambers for fission are used as transfer instruments. Participating laboratories have to produce quasi-monoenergetic neutrons of the desired energy and have to determine the accurate neutron fluence for the middle plane of the multiplate chambers. It is the fission-fragment rate above a certain threshold relative to this neutron-fluence rate which serves as transfer quantity.

Neutrons from the reactions $^7Li(p,n)$, T(p,n), D(d,n) were used at 0° and neutrons from the reaction T(d,n) at 74.4° for the energies 0.565, 2.5, 5.0 and 14.8 MeV, respectively. At all energies the determined neutron fluence refers to the n-p scattering. Recoil protons were detected quantitatively in a CH_4 filled proportional counter at 0.565 MeV and in a telescope coincidence counter (two ΔE, one E counter) for all other energies. The use of neutrons at 0° made it necessary to make the fluence determinations and the fission chamber measurements sequentially. Both kinds of runs were related by a source monitor which is a Cadarache directional counter positioned under 45° relative to the accelerator-beam direction at about 5.5 m distance.

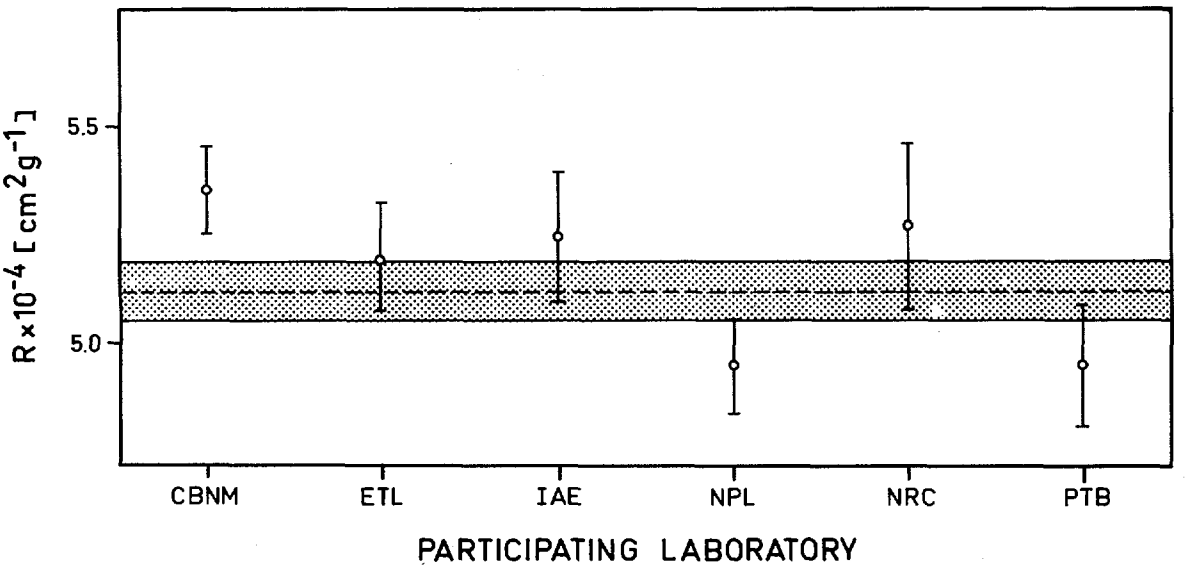

Fig. 32. Results of the intercomparison at 565 keV. The weighted mean is given by the hatched area

A schematic diagramme of the experimental set-up for fission-fragment counting with the multiplate-ionization chamber provided by the AERE, Harwell is shown in Fig. 33. A typical pulse-height spectrum as obtained with the ND 575 ADC on the right side in Fig. 33 is given in Fig. 34. Typical time-of-flight (TOF) spectra are shown in Fig. 35 (left side ND 575 ADC in Fig. 33). For data evaluation only coincident ADC signals were treated by the data acquisition system (128 x 128 channels). The average

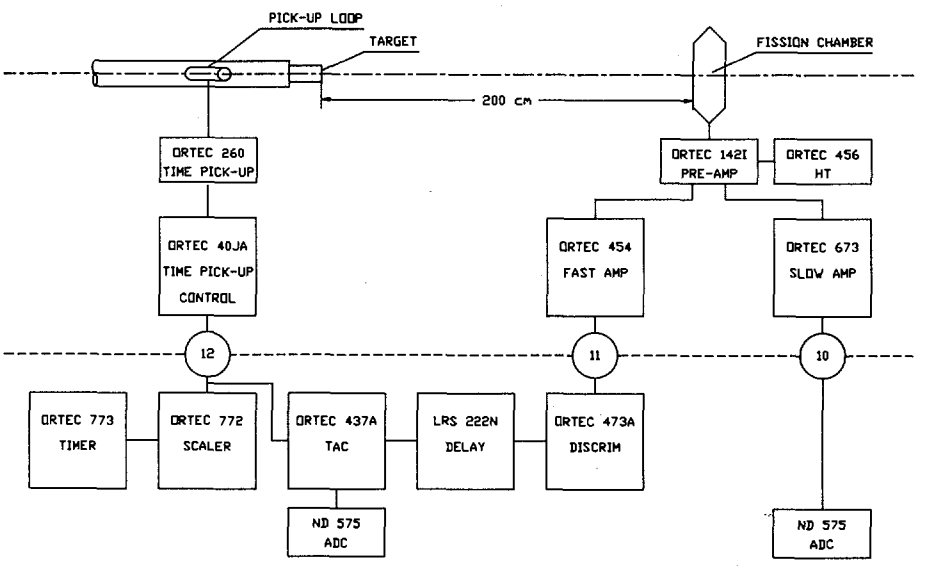

Fig. 33. Schematic diagramme of the electronic systems used for the extraction of pulse-height and timing signals

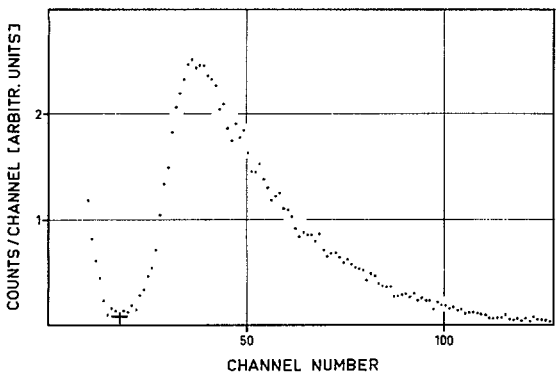

Fig.34. Typical fission fragment pulse-height spectrum observed with the ^{235}U ionization chamber.

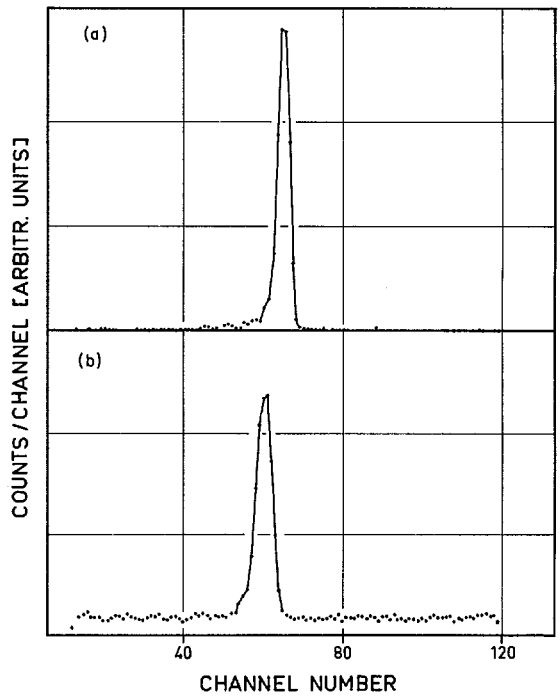

Fig.35. Typical TOF spectra (3.4 ns/channel) obtained at 5.0 MeV with the ^{235}U chamber (a) and at 2.5 MeV with the ^{235}U chamber (b)

accuracy of the fission-fragment rate above the pulse height indicated by a cross in Fig. 34, relative to the neutron fluence rate, was 2.9 %. The following corrections were taken into account: 1) dead time losses, 2) missing TOF stop pulses, 3) neutron inscattering, 4) spurious neutrons and 5) deviation from the nominal neutron energy. To ensure that the work for the intercomparison still going on in other laboratories is carried out under constant conditions the CBNM results will be reported only later.

TECHNICAL APPENDIX

Van de Graaff Accelerators

A. Crametz, P. Falque, J. Leonard, W. Schubert

A schematic view of both accelerators and the available beam tubes is shown in Fig. 36.

CN-7 MV machine: beam tubes, Cu-collimators and supports for the installation of a 40 m flight path on the R2 extension (30° right after switching magnet) have been ordered. The microcomputer hardware and software for the automatic control of the accelerator operation have been extended. Machine parameters can be logged and checked continuously. The accelerator will be shut down

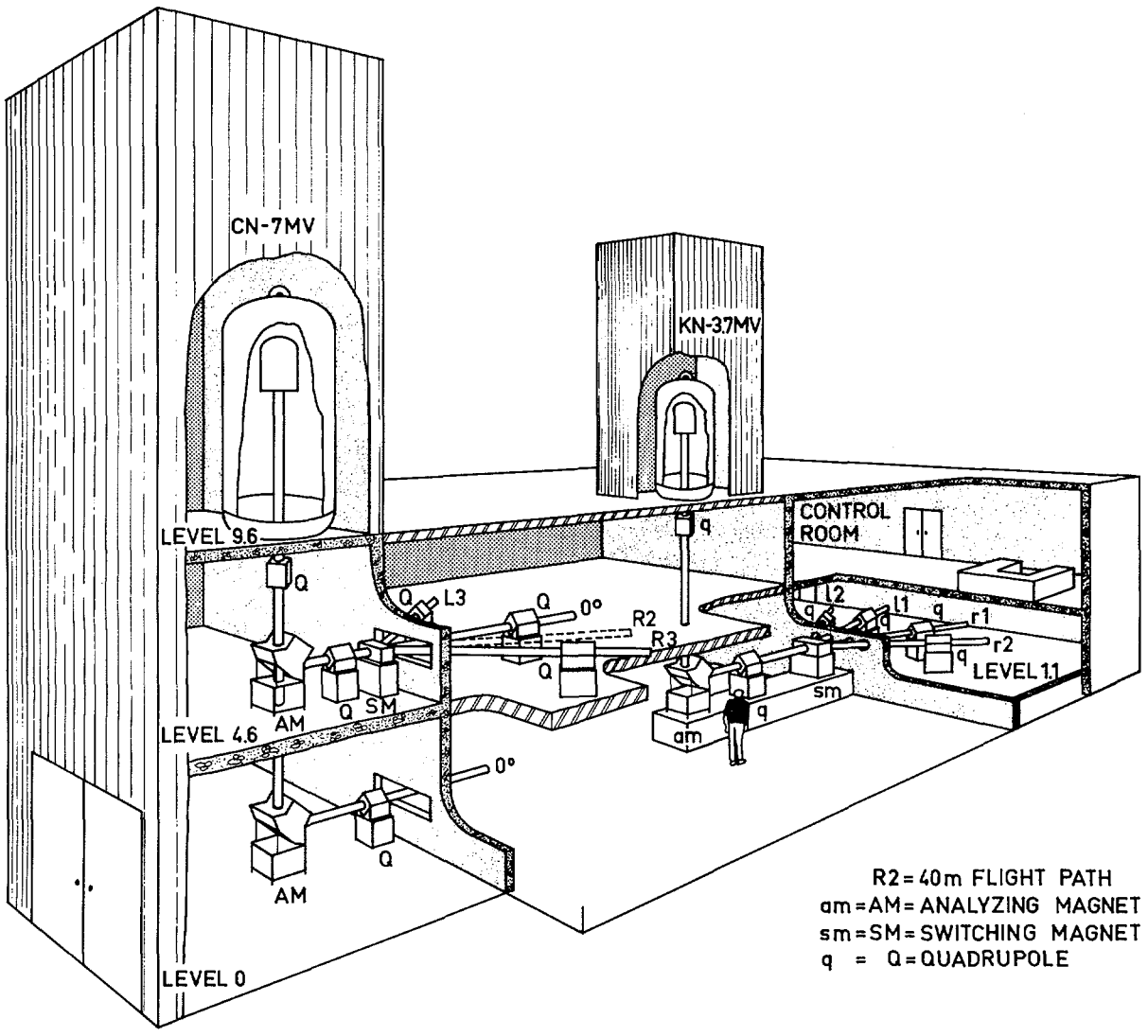

Fig. 36. CBNM - Van de Graaff accelerators

under computer control if certain parameters are passing predefined limits. In this way operator manpower can be saved.

KN-3.7 MV machine: to avoid that both accelerators fire into the same target hall, a second target site has been installed in the former machine room. This will improve the experimental conditions for future analytical ion-beam work, namely PIXE and RBS experiments. After modification of the machine and building infrastructure, the analyzing magnet has been moved from the 4.6 m level to that at 1.1 m, and the new beam optics have been calculated.

LIST OF PUBLICATIONS

CONTRIBUTIONS TO CONFERENCES

BAMBYNEK, W.
Statement on CBNM activity in evaluation and compilation of decay data.
IAEA Meeting on the Coordination of the International Network of Nuclear Structure and Decay Evaluations, Grenoble, June 2-5, 1986

BASTIAN, C.
The scope of APL in nuclear measurements.
APL 86, Manchester, July 6-11, 1986

BASTIAN, C.
EVAL: an interactive facility for multiparametric covariant evaluation.
IAEA Specialists Meeting on Covariance Methods and Practices in the Field of Nuclear Data, Rome, November 17-19, 1986

BÖCKHOFF, K.H.
Electron Linac based pulsed white sources for high resolution neutron time of flight spectroscopy - status and perspectives.
IAEA Advisory Group Meeting on Properties of Neutron Sources, Leningrad, June 9-13, 1986

BUDTZ-JØRGENSEN, C., KNITTER, H.-H.
Fragmentation and neutron emission for ^{252}Cf(sf).
Journées d'Etudes sur la Fission, Arcachon, October 14-17, 1986

BUDTZ-JØRGENSEN, C., KNITTER, H.-H., STRAEDE, Ch., HAMBSCH, F.-J.
Fragmentation for ^{235}U(n,f) and ^{252}Cf(sf).
Winter-Workshop on Nuclear Dynamics 4, Copper Mountain, Co., February 24-28, 1986

LISKIEN, H.
Neutron angular distributions from ^{7}Li.
IAEA Advisory Group Meeting on Nuclear Data for Fusion Reactor Technology, Gaussig/Dresden, December 1-5, 1986

PAUWELS, J., D'EER, A., NEVE DE MEVERGNIES, M., WAGEMANS, C., GÖNNEWEIN, F., GELTENBORT, P.
Thermal neutron induced fission of ^{235}U.
Journées d'Etudes sur la Fission, Arcachon, October 14-17, 1986

PAUWELS, J., EYKENS, R. D'EER, A., WAGEMANS, C., NEVE DE MEVERGNIES, M.
The realization of a ^{239}Pu mothersource for the preparation of ^{235m}U targets.
13th World Conference of the International Nuclear Target Development Society, Chalk River, September 17-19, 1986

REHER, D., WOODS, M.J., BALLAUX, C., NIJS, R., CELEN, E.
Construction of a stable air capacitor for use with standard ionization chambers.
ICRM Workshop on Ionization Chambers, Gaithersburg, November 19, 1986

WAGEMMANS, C., SCHILLEBEECKX, P., DERUYTTER, A., BARTHELEMY, R.
La fission spontanée et induite des isotopes du plutonium.
Journées d'Etudes sur la Fission, Arcachon, October 14-17, 1986

WEIGMANN, H.
Neutron spectroscopy with GELINA
Vth International School on Neutron Physics, Alushta, October 20-31, 1986

SCIENTIFIC OR TECHNICAL ARTICLES

AXTON, E.J.
The thermal neutron absorption cross sections of Mn and S.
Annals of Nucl. Energy 13 (1986) 627

BAMBYNEK, W.
Letter to the Editor: International Committee for Radionuclide Metrology.
Appl. Radiat. Isot. 37 (1986) 995

BÖCKHOFF, K., POORTMANS, F., SALOME, J.M.
The production and measuremnts of ultra-short intense electron and neutron bursts of GELINA.
Radiation Effects 95 (1986), 281

BRUSEGAN, A., BUYL, R., CORVI, F., MEWISSEN, L., POORTMANS, F., ROHR, G., SHELLEY, R., VAN DER VEEN, T., VAN MARCKE, I.
High resolution neutron capture and total cross section measurements of ^{50}Cr and ^{53}Cr.
Radiation Effects 93 (1986) 297

BUDTZ-JØRGENSEN, C., KNITTER, H.-H.
Fragmentation and neutron emission for ^{252}Cf
Proc. Seminar on Fission, Habay-la-Neuve, BLG-586 (1986), p. 91

BUDTZ-JØRGENSEN, C., KNITTER, H.-H.
Correlation between neutron and fragments in ^{252}Cf (sf).
Radiation Effects 93 (1986) 5

CORVI, F., BASTIAN, C., WISSHAK, K.
Neutron capture in the 1.15 keV resonance of ^{56}Fe using Moxon-Rae detectors.
Nucl. Sci. Eng. 93 (1986) 348

COURSEY, B.M., MANN, W.B., GRAU MALONDA, A., GARCIA TORANO, E., LOS ARCOS, J.M., GIBSON, J.A.B., REHER, D.
Standardization of carbon-14 by $4\pi\beta$ liquid scintillation efficiency tracing with hydrogen-3.
Appl. Radiat. Isot. 37 (1986) 403

CRAMETZ, A., DE JONGE, S., LISKIEN, H., JAESCHLE, E., INGWERSEN, H.
Post acceleration bunching system for a CN-type Van de Graaff accelerator.
Nucl. Instrum. Methods Phys. Res. A242 (1986) 179

DEBUS, G.H., HANSEN, H.H. (eds.)
Annual Progress Report on Nuclear Data 1985.
NEANDC (E) 272 "U", Vol. III EURATOM; INDC (EUR) 020/G, 1986

DEKEMPENEER, E., LISKIEN, H., MEWISSEN, L., POORTMANS, F.
A spectrometer for double-differential neutron-emission cross section measurements.
Proc. Intern. Conf. on Fast Neutron Physics, Dubrovnik (1986), p. 227

DERUYTTER, A.
Fission revisited, keynote address.
Proc. Seminar on Fission, Habay-la-Neuve, BLG-586 (1986), p. 6

HAMBSCH, F.-J., KNITTER, H.-H., BUDTZ-JØRGENSEN, C., THEOBALD, J.P.
Untersuchung zur Neutronen induzierten Spaltung von ^{235}U im Energiebereich von thermisch bis 6 MeV.
Verhandlungen der Deutschen Physikalischen Gesellschaft, 4 (1986) 135

JANSSENS, A., COTTENS, E., PAULSEN, A., POFFIJN, A.
Equilibration of a graphite absorbed-dose calorimeter and the quasi-isothermal mode of operation.
Metrologia 22 (1986) 265

KÖHLER, R., MEWISSEN, L., POORTMANS, F., RAMAN, S., WARTENA, J.A., WEIGMANN, H.
Doorways in the reaction $^{207}Pb+n$.
Radiation Effects 94 (1986) 231

LISKIEN, H.
Angular distribution for $^{7}Li(n,n')^{7}Li^{*}(478)$ by analysing Doppler-broadened γ lines.
Radiation Effects 94 (1986) 271

LISKIEN, H., BAO, S.
$^{7}Li(n,n')^{7}Li^{*}(478)$ neutron angular distribution derived from Doppler broadened γ-energy distributions.
Proc. Intern. Conf. on Fast Neutron Physics, Dubrovnik (1986), p. 275

QUAIM, S., WÖLFLE, R., LISKIEN, H.
Excitation function of $^{93}Nb(n, {}^{3}He)^{91}Y$ reaction near its threshold: comparison of ^{3}He and ^{3}H emission probabilites.
Phys. Rev. C34 (1986) 489

REHER, D., HANSEN, H.H., VANINBROUKX, R., WOODS, M.J., GRANT, C.E., LUCAS, S.E.M., BOUCHARD, J., MOREL, J., VATIN, R.
The decay of ^{47}Sc.
Appl. Radiat. Isot. 37 (1986) 973

ROHR, G.
Die Eigenschaften von Intruder-Zuständen untersucht an Cadmium-Isotopen.
Verhandlungen der Deutschen Physikalischen Gesellschaft, 4 (1986) 502

SALOME, J.M.
GELINA, l'accelérateur à électrons du BCMN.
Physicalia Magazine 8 (1986) 261

SCHILLEBEECKX, P., WAGEMANS, C., DERUYTTER, A., BARTHELEMY, R.
Fission fragment energy and mass distributions in the spontaneous fission of the Pu isotopes.
Proc. Seminar on Fission, Habay-la-Neuve, BLG-586 (1986), p. 124

STRAEDE, Ch., BUDTZ-JØRGENSEN, C., KNITTER, H.-H.
^{235}U(n,f) fragment mass, kinetic energy, angular distribution and cold fragmentation.
Proc. Seminar on Fission, Habay-la-Neuve, BLG-586 (1986), p. 140

VANINBROUKX, R., BORTELS, G., DENECKE, B.
Alpha-particle and gamma-ray emission probabilities in the decay of ^{242}Pu.
Appl. Radiat. Isot. 37 (1986) 1167

VAN PRAET, G., CORNELIS, E., RAMAN, S., ROHR, G.
Neutron capture measurements on ^{241}Am
Radiation Effects 93 (1986) 157

WAGEMANS, C., DERUYTTER, A.
Subthermal fission cross-section measurements.
Radiation Effects 93 (1986) 163

WATTECAMPS, E., ARNOTTE, F.
Measurements from 5 to 10 MeV of double-differential (n,α) cross sections of Ni and Cu.
Proc. Intern. Conf. on Fast Neutron Physics, Dubrovnik (1986), p. 258

WEIGMANN, H.
Recent advances and future trends in neutron resonance spectroscopy.
Radiation Effects 94 (1986) 179

WEIGMANN, H.
Neutron induced fission below and at the fission barrier.
Proc. Seminar on Fission, Habbay-la-Neuve, BLG-586 (1986), p. 32

SPECIAL PUBLICATIONS

BAMBYNEK, W.
^{241}Am: Emission probabilities of selected gamma rays.
Decay Data of the Transactinium Nuclides, Technical Reports Series N° 261, IAEA, Vienna (1986), p. 128

VANINBROUKX, R.
^{235}U: Emission probabilities of selected gamma rays.
Ibidem, p. 69

VANINBROUKX, R.
^{239}Np: Emission probabilities of selected gamma rays.
Ibidem, p. 89

VANINBROUKX, R.
^{239}Pu: Half-life.
Ibidem, p. 99

VANINBROUKX, R.
^{242}Pu: Emission probabilities of selected gamma rays.
Ibidem, p. 121

VANINBROUKX, R.
^{241}Am: Half-life.
Ibidem, p. 127

VANINBROUKX, R.
^{243}Am: Half-life, II. Emission probabilities of selected gamma rays.
Ibidem, p. 137

REICH, C.W., VANINBROUKX, R.
Current status on nuclear decay data and report on the IAEA coordinated research programme on the measurement and evaluation of transactinium isotope nuclear decay data.
EGG-2466 (1986)

GLOSSARY

A E C L	Atomic Energy of Canada Limited, Chalk River (Canada)
A E R E	Atomic Energy Research Establishment, Harwell (GB)
A G M	Advisory Group Meeting
B I P M	Bureau International des Poids et Mesures, Paris (F)
C B N M	Central Bureau for Nuclear Measurements (JRC-Geel), Geel (B)
C C E M R I	Comité Consultatif pour les Etalons de Mesure des Rayonnements Ionisants
C E A	Commissariat à L'Energie Atomique, Paris (F)
C I E M A T - J E N	Centro de Investigacion Energetica Medio Ambiental y Tecnologia - Junta de Energia Nuclear, Madrid (E)
C N R S	Centre National de la Recherche Scientifique, Orléans (F)
D W B A	Distorted Wave Born Approximation
E C N	Energieonderzoek Centrum Nederland, Petten (NL)
E N D F	Evaluated Nuclear Data File
E P F L	Ecole Polytechnique Fédérale de Lausanne, Lausanne (CH)
E T L	Electronical Laboratory, Ibaraki (Japan)
E X F O R	Exchange Format
F W H M	Full Width at Half Maximum
G E L I N A	Geel Electron Linear Accelerator
G K S S	Gesellschaft für Kernergieverwertung in Schiffbau und Schiffahrt mbH, Geesthacht (D)
I A E A	International Atomic Energy Agency, Vienna (A)
I E A	Instytut Energii Atomowej, Swierk (PL)
I E R	Institut d'Electrochimie et Radiochimie de l'EPFL, Lausanne (CH)
I C R M	International Committee for Radionuclide Metrology
I L L	Institut Laue-Langevin, Grenoble (F)
I M M	Institut de Métrologie D.I. Mendéléev, Leningrad (SU)
I N D C	International Nuclear Data Committee
I P E N	Instituto de Pesquisas Energeticas e Nucleares, Sao Paulo (Brazil)
J E F	Joint European File
J E N D L	Japanese Evaluated Nuclear Data Library
J R C	Joint Research Centre
K F A	Kernforschungsanlage, Jülich (D)
K F K	Kernforschungszentrum Karlsruhe, Karlsruhe (D)

K S R I	Korean Standards Research Institute, Taejou (Korea)
L A N L	Los Alamos National Laboratory, Los Alamos (USA)
L M R I	Laboratoire de Métrologie des Rayonnements Ionisants, Saclay (F)
N A C	National Accelerator Centre, Faure (F)
N B S	National Bureau of Standards, Gaithersburg (U S A)
N E A	Nuclear Energy Agency, Paris (F)
N E A C R P	Nuclear Energy Agency's Committee for Reactor Physics
N E A N D C	Nuclear Energy Agency's Nuclear Data Committee
N I M	National Institute of Metrology, Beijing (PR of China)
N P L	National Physical Laboratory, Teddington (GB)
O M H	Országos Mérésügyi Hivatal, Budapest (H)
O R N L	Oak Ridge National Laboratory, Oak Ridge (USA)
P I X E	Particle Induced X-ray Emission
P T B	Physikalisch-Technische Bundesanstalt, Braunschweig (D)
R B S	Rutherford Backscattering
S C K/ C E N	Studiecentrum voor Kernenergie/ Centre d'Etudes Nucleaires, Mol (B)
S I R	Système International de Référence
T R C	The Radiochemical Centre, Amersham (GB)
U V V V R	Ústavu pro Výzkum, Výrobu a Využití Radioisotopu, Prague (CS)
W R E N D A	World Request List for Neutron Data Measurements

CINDA ENTRIES LIST

ELEMENT		QUANTITY	TYPE	ENERGY		DOCUMENTATION		LAB	COMMENTS
S	A			MIN	MAX	REF VOL PAGE	DATE		
LI	007	DIN	EXPTL-PROG	40 + 6	10 + 7	INDC(EUR)21G 29	687	GEL	LISKIEN + VDG
LI	007	NEM	EXPTL-PROG	10 + 6	90 + 6	INDC(EUR)21G 30	687	GEL	LISKIEN + LINAC DBLEDIFF
BE	009	NEM	EXPTL-PROG	10 + 6	90 + 6	INDC(EUR)21B 34	687	GEL	DEKEMPENEER + LINAC DBLEDIFF
BE	009	NT	EXPTL-PROG	14 + 7		INDC(EUR)21G 34	687	GEL	LISKIEN + VDG TRITIUM COUNTING
SI	028	RES	EXPTL-PROG	30 + 4	30 + 6	INDC(EUR)21G 38	687	GEL	MARTIN + LINAC
S	033	NA	EXPTL-PROG	20-2	10 + 6	INDC(EUR)21G 39	687	GEL	WAGEMANS + LINAC
CR	050	RES	EXPTL-PROG	00 + 0	80 + 5	INDC(EUR)21G 42	687	GEL	ROHR + LINAC TRANSM
NI		NA	EXPTL-PROG	50 + 6	10 + 7	INDC(EUR)21G 36	687	GEL	WATTECAMPS + VDG RATIO NI60/NI58
PB	207	RES	EXPTL-PROG	30 + 4	70 + 5	INDC(EUR)21G 39	687	GEL	KOEHLER + LINAC
U	235	FRS	EXPTL-PROG	30-2	50 + 5	INDC(EUR)21G 05	687	GEL	KNITTER + LINAC MASS, ANG DIST
U	235	NF	EXPTL-PROG	10-3	10 + 1	INDC(EUR)21G 19	687	GEL	WAGEMANS + LINAC REL TO LI6NT
U	235	ETA	EXPTL-PROG	20-3	30-1	INDC(EUR)21G 20	687	GEL	WEIGMANN + LINAC
PU	236	FRS	EXPTL-PROG			INDC(EUR)21G 21	687	GEL	WAGEMANS + SPONTFISS
PU	239	NF	EXPTL-PROG	10-3	10 + 1	INDC(EUR)21G 19	687	GEL	WAGEMANS + LINAC REL TO LI6NT
AM	243	NF	EXPTL-PROG	10 + 0	10 + 7	INDC(EUR)21G 21	687	GEL	KNITTER + LINAC, VDG
CF	252	SFN	EXPTL-PROG			INDC(EUR)21G 10	687	GEL	BUDTZ-JØRGENSEN + SF ANG, MASS DIST